

Primordial non-Gaussianity from a joint analysis of the cosmic microwave background temperature and polarization

Article (Published Version)

Munshi, Dipak, Coles, Peter, Cooray, Asantha, Heavens, Alan and Smidt, Joseph (2011) Primordial non-Gaussianity from a joint analysis of the cosmic microwave background temperature and polarization. *Monthly Notices of the Royal Astronomical Society*, 410 (2). pp. 1295-1319. ISSN 0035-8711

This version is available from Sussex Research Online: <http://sro.sussex.ac.uk/id/eprint/44526/>

This document is made available in accordance with publisher policies and may differ from the published version or from the version of record. If you wish to cite this item you are advised to consult the publisher's version. Please see the URL above for details on accessing the published version.

Copyright and reuse:

Sussex Research Online is a digital repository of the research output of the University.

Copyright and all moral rights to the version of the paper presented here belong to the individual author(s) and/or other copyright owners. To the extent reasonable and practicable, the material made available in SRO has been checked for eligibility before being made available.

Copies of full text items generally can be reproduced, displayed or performed and given to third parties in any format or medium for personal research or study, educational, or not-for-profit purposes without prior permission or charge, provided that the authors, title and full bibliographic details are credited, a hyperlink and/or URL is given for the original metadata page and the content is not changed in any way.

Primordial non-Gaussianity from a joint analysis of the cosmic microwave background temperature and polarization

Dipak Munshi,^{1,2★} Peter Coles,¹ Asantha Cooray,³ Alan Heavens² and Joseph Smidt³

¹*School of Physics and Astronomy, Cardiff University, Queen's Buildings, 5, The Parade, Cardiff CF24 3AA*

²*Scottish Universities Physics Alliance (SUPA), Institute for Astronomy, University of Edinburgh, Blackford Hill, Edinburgh EH9 3HJ*

³*Department of Physics and Astronomy, University of California, Irvine, CA 92697, USA*

Accepted 2010 August 12. Received 2010 August 12; in original form 2010 March 5

ABSTRACT

We explore a systematic approach to the analysis of primordial non-Gaussianity using fluctuations in the temperature and polarization of the cosmic microwave background (CMB). Following Munshi & Heavens, we define a set of power spectra as compressed forms of the bispectrum and trispectrum derived from CMB temperature and polarization maps; these spectra compress the information content of the corresponding full multispectra and can be useful in constraining early Universe theories. We generalize the standard pseudo- C_l estimators in such a way that they apply to these spectra involving both spin-0 and spin-2 fields, developing explicit expressions, which can be used in the practical implementation of these estimators. While these estimators are suboptimal, they are nevertheless unbiased and robust and hence can provide useful diagnostic tests at a relatively small computational cost. We next consider approximate inverse-covariance weighting of the data and construct a set of near-optimal estimators based on that approach. Instead of combining all available information from the entire set of mixed bi- or tri-spectra, that is, multispectra describing both temperature and polarization information, we provide analytical constructions for individual estimators, associated with particular multispectra. The bias and scatter of these estimators can be computed using Monte Carlo techniques. Finally, we provide estimators, which are completely optimal for arbitrary scan strategies and involve inverse-covariance weighting; we present the results of an error analysis performed using a Fisher-matrix formalism at both the one-point and two-point levels.

Key words: methods: analytical – methods: numerical – methods: statistical – cosmic background radiation – large-scale structure of Universe.

1 INTRODUCTION

The cosmic microwave background (CMB) has the potential to provide cosmologists with the cleanest statistical characterization of primordial fluctuations. In most early universe studies, the primordial fluctuations are assumed to be nearly Gaussian, but the quest for an experimental detection of primordial non-Gaussian is of considerable importance. Early observational work on the bispectrum from *COBE* (Komatsu et al. 2002) and *MAXIMA* (Santos et al. 2003) was followed by much more accurate analysis using data from the *Wilkinson Microwave Anisotropy Probe* (*WMAP*)¹ (Komatsu et al. 2003; Creminelli et al. 2007; Spergel et al. 2007). With the recent claim of a detection of non-Gaussianity (Yadav & Wandelt 2008) in the 5-yr *WMAP* data, interest in non-Gaussianity has received a tremendous boost. However, these, and most other, studies of primordial non-Gaussianity focus primarily on data relating to temperature anisotropies, whereas inclusion of E-polarization data could, in principle, increase the sensitivity of such tests. Ongoing surveys, such as that derived from the *Planck* Surveyor,² will throw more light on this question by improving sensitivity to both temperature and polarization fluctuations. It is the primary purpose of this paper to extend a number of previously obtained analytical results in order to design a new set of diagnostic tools for the analysis of primordial non-Gaussianity using both temperature and polarization data.

★E-mail: Dipak.Munshi@astro.cf.ac.uk

¹ <http://map.gsfc.nasa.gov/>

² <http://www.rssd.esa.int/index.php?project=Planck>

The CMB polarization field can be decomposed into a gradient part with even parity (the ‘electric’ or E mode) and a curl part with odd parity (the ‘magnetic’ or B mode), with important ramifications for its interpretation in a cosmological setting. Scalar (density) perturbations, at least in the linear regime, are unable to generate B-mode polarization directly. Secondary effects, such as gravitational lensing, can generate magnetic polarization from an initial purely electric type, but only on relatively small angular scales. Tensor (gravitational-wave) perturbations, however, can generate both the E and B modes on large scales. Detection of B-mode polarization on large angular scales is therefore, at least in principle, a tell-tale signature of the existence of gravitational waves predicted to be generated during inflation. The amplitude of these tensor perturbations also contains information relating to the energy scale of inflation and thus has considerable power to differentiate among alternative models of the early Universe.

A number of experiments therefore are either being planned or currently underway to characterize the polarized CMB sky, including *Planck*. The primary statistical tools currently used to characterize the stochastic polarized component are the power spectra of the E- and B-mode contributions; these have been studied in the literature in great detail for various survey strategies, non-uniform noise distribution, and partial sky coverage (Hivon et al. 2002). Most studies in this vein involve a (computationally extensive) maximum-likelihood analysis or a quadratic estimator, which has limited ability to handle maps with large numbers of pixels, or the so-called pseudo- C_l estimator (PCL), which uses a heuristic weighting of various pixels, instead of an optimal or near-optimal one.

Information about non-Gaussianity, however, is not contained in the power spectrum C_l ; however, it is estimated. A recent study by Munshi et al. (2009) extended the PCL approach to the study of non-Gaussianity by taking into account higher order spectra, as well as clarifying the relationship of the estimators obtained to the optimal ones. This was done for temperature only, so one of the aims of this paper is to generalize this early work to take into account both temperature and polarization.

Approaches based on PCL do not require detailed theoretical modelling of the target bispectrum. Optimal estimators, on the other hand, work using a matched-filter approach, which does require analytical modelling. The simplest inflationary models – based on a single slowly rolling scalar field – are associated with a very small level of non-Gaussianity (Salopek & Bond 1990, 1991; Falk et al. 1993; Gangui et al. 1994; Acquaviva et al. 2003; Maldacena 2003; Linde & Mukhanov 1997; Bartolo et al. 2006, and references therein for more details). More elaborate variations on the inflationary theme, such as those involving multiple scalar fields (Lyth, Ungarelli & Wands 2003), features in the inflationary potential, non-adiabatic fluctuations, non-standard kinetic terms, warm inflation (Gupta, Berera & Heavens 2002; Moss & Xiong 2007) or deviations from Bunch–Davies vacuum, can lead to much higher level of non-Gaussianity.

Generally speaking, the apparatus used to model primordial non-Gaussianity has focused on a phenomenological ‘local f_{NL} ’ parametrization in terms of the perturbative non-linear coupling in the primordial curvature perturbation (Komatsu & Spergel 2001):

$$\Phi(x) = \Phi_L(x) + f_{\text{NL}} [\Phi_L^2(x) - \langle \Phi_L^2(x) \rangle] + g_{\text{NL}} \Phi_L^3(x) + \dots, \quad (1)$$

where $\Phi_L(x)$ denotes the linear Gaussian part of the Bardeen curvature (Bartolo et al. 2006) and f_{NL} is the non-linear coupling parameter. A number of models have non-Gaussianity, which can be approximated by this form. The leading order non-Gaussianity therefore is at the level of the bispectrum or, equivalent, at the three-point level in configuration space. Many studies involving primordial non-Gaussianity have used the bispectrum, motivated by the fact that it contains all the information about f_{NL} (Babich 2005). This has been extensively studied (Creminelli 2003; Komatsu, Spergel & Wandelt 2005; Cabella et al. 2006; Creminelli et al. 2006; Medeiros & Contaldo 2006; Liguori et al. 2007; Smith, Senatore & Zaldarriaga 2009), with most of these measurements providing convolved estimates of the bispectrum. Optimized three-point estimators were introduced by Heavens (1998) and have been successively developed (Komatsu et al. 2005; Smith, Zahn & Dore 2007; Creminelli et al. 2006; Smith & Zaldarriaga 2006; Creminelli, Senatore & Zaldarriaga 2007) to the point, where an estimator for f_{NL} , which saturates the Cramer–Rao bound exists for partial sky coverage and inhomogeneous noise (Smith et al. 2009). Approximate forms also exist for *equilateral* non-Gaussianity, which may arise in models with non-minimal Lagrangian with higher derivative terms (Chen et al. 2007a; Chen, Easther & Lim 2007b). In these models, the largest signal comes from spherical harmonic modes with $\ell_1 \simeq \ell_2 \simeq \ell_3$, whereas for the local model, the signal is highest when one ℓ is much smaller than the other two. Moreover, the covariances associated with these power spectra can be computed analytically for various models, thereby furnishing methods to test simulation pipeline in a relatively cost-effective way.

As mentioned above, most of the analyses of the CMB bispectrum take into account only temperature information because of lower sensitivity associated with polarization measurements. However, the overall signal-to-noise ratio (S/N) of a detection of non-Gaussianity can, in principle, be improved by incorporating E-type polarization information in a joint analysis. Several ground-based or future experiments³ have either started or will be measuring E polarization, and ongoing all-sky experiments, such as *Planck*, will certainly improve the S/N. Moreover, there are many planned experiments, which will survey the sky with even better sensitivity (see e.g. Baumann et al. 2009 for the CMBPol mission concept study). It is therefore clearly timely to update and upgrade the available estimators, which can analyse both temperature and polarization. The main question is how to do it optimally.

The fast estimator introduced initially by Komatsu et al. (2005) can handle temperature and polarization data. Extension of this estimator to take into account a linear term, which can reduce the variance in the presence of partial sky coverage, was introduced later in Creminelli et al. (2006). In the absence of a linear term, the scatter associated with the estimator increases at high ℓ . A more general approach, that includes inverse-variance weighting of the data, was introduced by Smith & Zaldarriaga (2006), which can make the estimator optimal.

³ See e.g. <http://cmbpol.uchicago.edu/workshops/path2009/abstracts.html> for various ongoing and planned surveys.

However, most of these estimators tend to compress all available information into a single point. This has the advantage of reducing the scatter in the estimator, but it throws away a great deal of potentially relevant information.

Recently, Munshi & Heavens (2010) have extended this approach by devising a method, which can map the bispectrum, or even higher order spectra, such as the trispectrum, to associated power spectra; these power spectra are related to the *cumulant correlators* used in the context of projected galaxy surveys (Szapudi & Szalay 1999; Munshi, Melott & Coles 2000). These compressed spectra do not contain all the information contained in the multispectra, but they certainly do carry more information than a single number, and for certain purposes, such as f_{NL} estimation, can be completely optimal.

In this paper, we extend the analysis of Munshi & Heavens (2010) to the case of a joint analysis of temperature and E-mode polarization data. We provide realistic estimators for power spectra related to *mixed* bispectra and trispectra (i.e. multispectra incorporating and describing both temperature and polarization properties of the radiation field) in the presence of partial sky coverage. We then generalize these results to the case of optimized estimators, which can handle all realistic complications by an appropriate optimal weighting of the data. We also provide a detailed analysis of pseudo- C_ℓ based estimators. Though suboptimal, these estimators are unbiased and turn out to be valuable diagnostics for analysing large number of simulations very quickly.

This paper is organized as follows. In Section 2, we describe the basic results needed for the PCL analysis. We then introduce the power spectrum associated with the mixed bispectrum. The formalism is sufficiently general to handle both E and B modes, but for simplicity and practical relevance, we give results for the E mode only. These results are next generalized in Section 4 to near-optimal estimators, which were introduced by Komatsu et al. (2005). The optimization depends on matched-filtering techniques based on theoretical modelling of primordial non-Gaussianity presented in Section 3 and relies on Monte Carlo (MC) standardization of bias and scatter. Next, we consider the approach, where various fields are weighted by inverse-covariance matrices to make them optimal in Section 5. Though this approach does not rely on MC simulations, accurate modelling of inverse-covariance matrix can be computationally expensive and can only be achieved for maps with relatively low resolution.

2 METHOD OF DIRECT INVERSION OR PSEUDO- C_ℓ APPROACH

Maximum-likelihood analysis techniques, or related quadratic estimators, are generally used to estimate the power spectrum from a given cosmological data set, such as a map of the CMB. This approach relies on (optimal) inverse-covariance weighting of the data which, unfortunately, is virtually impossible to implement in practice for large data sets. However, faster *direct* inversion techniques with heuristic weighting schemes are faster and are typically employed for estimation of power spectra from cosmological data (Hivon et al. 2002). The alternative, PCL, technique discussed above can, however, be used to study the power spectrum related to the bispectrum. This method is not optimal, but remains unbiased and can act as a precursor to more computationally expensive studies using various optimal estimators.

This section is devoted to the generalization of the PCL results to the *skew spectrum* associated with spinorial fields, such as polarization radiation. The results we shall derive are valid for all-sky coverage as well as for partial sky coverage; we relate the two using a coupling matrix, which depends on the power spectrum associated with the mask describing the coverage. We provide results for the coupling matrix for various generic combinations of spin-0 and spin-2 fields. These results extend the results obtained previously for the temperature-only case (spin 0).

2.1 The power spectrum associated with the bispectrum

We start by defining the complex field $P_\pm(\hat{\Omega})$ constructed from the Stoke's parameters $Q(\hat{\Omega})$ and $U(\hat{\Omega})$:

$$P_\pm(\hat{\Omega}) = Q(\hat{\Omega}) \mp iU(\hat{\Omega}). \quad (2)$$

The fields denoted $P_\pm(\hat{\Omega})$ are spin-2 (tensor) fields, whereas the temperature field can be represented as a spin-0 (scalar) field on the surface of the sky. The appropriate multipole expansion of these objects is performed using the *spin-2 spherical harmonics*, $_{\pm 2}Y_{lm}$, as basis functions. We will denote the spin harmonics of spin s with $_sY_{lm}(\hat{\Omega})$ on the surface of a unit sphere:

$$P_\pm(\hat{\Omega}) = \sum_{lm} \mp 2 Y_{lm}(\hat{\Omega}) (E_{lm} \pm B_{lm}); \quad [P_\pm]_{lm} = (E_{lm} \pm B_{lm}). \quad (3)$$

The terms E_{lm} and B_{lm} are the harmonic components of *electric* and *magnetic* components, respectively. It should be clear that the fields P_\pm , constructed from Q and U , correspond to spin ∓ 2 , respectively.

Estimation of power spectra for the E and B fields from experiments with partial sky coverage is of great importance for cosmological experiments and has attracted a great deal of interest.

We start by considering two fields on the surface of a sphere $\mathcal{X}(\hat{\Omega})$ and $\mathcal{Y}(\hat{\Omega})$, which are, respectively, of spin x and y . These objects can be P_\pm or δT . Resulting product fields, such as P_+P_- , can be of spin 0, while those like P_+^2 and P_-^2 are of spin -4 and $+4$, respectively. The results can also involve fields, such as $\delta_T P_+$, which is a spin -2 field. All these spin- s fields can be decomposed using spin harmonics $_sY_{lm}(\hat{\Omega})$ given above. These spin harmonics are generalization of ordinary spherical harmonics $Y_{lm}(\hat{\Omega})$, which are used to decompose the spin-0 (or scalar) functions, for example, δT defined over a surface of the celestial sphere. Throughout we will be using lower-case symbols x, y to denote the spins associated with the corresponding fields denoted in italics. The fields that are constructed from various powers of P_+ and P_- can be expanded in terms of the corresponding spin-harmonics basis $_sY_{lm}(\hat{\Omega})$. The product field, such as $[\mathcal{X}(\hat{\Omega})\mathcal{Y}(\hat{\Omega})]$, which is of

spin $x + y$ can therefore be expanded in terms of the harmonics $_{x+y}Y_{lm}(\hat{\Omega})$. The following relationship therefore expresses the harmonics of the product field in terms of the harmonics of individual fields:

$$[\mathcal{X}(\hat{\Omega})\mathcal{Y}(\hat{\Omega})]_{lm} = \int d\hat{\Omega} \mathcal{X}(\hat{\Omega})\mathcal{Y}(\hat{\Omega}) [_{x+y}Y_{lm}^*(\hat{\Omega})] \quad (4)$$

$$\sum_{l_i m_i} \mathcal{X}_{l_1 m_1} \mathcal{Y}_{l_2 m_2} \int [_{x}Y_{l_1 m_1}(\hat{\Omega})][_{y}Y_{l_2 m_2}(\hat{\Omega})] [_{x+y}Y_{lm}^*(\hat{\Omega})] d\hat{\Omega}; \quad \mathcal{X}, \mathcal{Y} \in P_{\pm} \quad (5)$$

$$= \sum_{l_i m_i} \mathcal{X}_{l_1 m_1} \mathcal{Y}_{l_2 m_2} I_{l_1 l_2 l} \begin{pmatrix} l_1 & l_2 & l \\ x & y & -(x+y) \end{pmatrix} \begin{pmatrix} l_1 & l_2 & l \\ m_1 & m_2 & -m \end{pmatrix}; \quad I_{l_1 l_2 l} = \sqrt{\frac{(2l_1+1)(2l_2+1)(2l+1)}{4\pi}}. \quad (6)$$

The expression derived above is valid for all-sky coverage; it will be generalized later to take into account arbitrary partial sky coverage. We have assumed that any noise contamination is Gaussian, so that it will not contribute to this non-Gaussianity statistic. To define the associated power spectra, we can write

$$C_l^{\mathcal{X}\mathcal{Y}, \mathcal{Z}} = \frac{1}{2l+1} \sum_m [\mathcal{X}\mathcal{Y}]_{lm} Z_{lm}^* = \sum_{l_1 l_2} B_{l_1 l_2 l}^{\mathcal{X}\mathcal{Y}\mathcal{Z}} \sqrt{\frac{(2l_1+1)(2l_2+1)}{(2l+1)}} \begin{pmatrix} l_1 & l_2 & l \\ x & y & -(x+y) \end{pmatrix}. \quad (7)$$

Here, we have introduced the bispectrum $B_{l_1 l_2 l}^{\mathcal{X}\mathcal{Y}\mathcal{Z}}$, which can be related to the harmonics of the relevant fields by the following equation:

$$B_{l_1 l_2 l_3}^{\mathcal{X}\mathcal{Y}\mathcal{Z}} = \sum_{m_1 m_2 m_3} \langle \mathcal{X}_{l_1 m_1} \mathcal{Y}_{l_2 m_2} \mathcal{Z}_{l_3 m_3} \rangle_c \begin{pmatrix} l_1 & l_2 & l_3 \\ m_1 & m_2 & m_3 \end{pmatrix}. \quad (8)$$

The matrices denote the Wigner-3j symbols (Edmonds 1968), which are only non-zero when the quantum numbers l_i and m_i satisfy certain conditions. For $x = y = 0$, these results generalize those obtained in Cooray (2001) valid for the case of temperature; see also Chen & Szapudi (2006) for related discussions. The result derived above is valid for a general E- and B-type polarization field. The contribution from B-type magnetic polarization is believed to be considerably smaller than the E-type electric polarization. The results derived above will simplify considerably, if we ignore the B-type polarization field in our analysis. In general, the power spectra described above will be complex functions, though the real and imaginary parts can be separated by considering different components of the bispectrum. However, if we assume that the magnetic part of the polarization is zero, then the following equalities will hold:

$$B_{l_1 l_2 l_3}^{\delta T \delta T \delta T} = B_{l_1 l_2 l_3}^{TTT}; \quad B_{l_1 l_2 l_3}^{P_{\pm} \delta T \delta T} = B_{l_1 l_2 l_3}^{ETT}; \quad B_{l_1 l_2 l_3}^{P_{\pm} P_{\pm} \delta T} = B_{l_1 l_2 l_3}^{EET}; \quad B_{l_1 l_2 l_3}^{P_{\pm} P_{\pm} P_{\pm}} = B_{l_1 l_2 l_3}^{EEE}. \quad (9)$$

The result detailed above is valid for all-sky coverage. Clearly, for our results to be relevant in practical applications, we need to add a Galactic mask. If we construct the masked harmonics associated with an (arbitrary) mask $w(\hat{\Omega})$, then, expanding the product field in the presence of the mask, we can write

$$\begin{aligned} [\mathcal{X}(\hat{\Omega})\mathcal{Y}(\hat{\Omega})w(\hat{\Omega})]_{lm} &= \sum_{l_i m_i} \mathcal{X}_{l_1 m_1} \mathcal{Y}_{l_2 m_2} w_{l_a m_a} \int [_{x}Y_{l_1 m_1}(\hat{\Omega})][_{y}Y_{l_2 m_2}(\hat{\Omega})][_{l_a m_a}Y_{lm}^*] d\hat{\Omega} \\ &= \sum_{l_i m_i} \sum_{l_a m_a} (-1)^{l'} \mathcal{X}_{l_1 m_1} \mathcal{Y}_{l_2 m_2} w_{l_a m_a} I_{l_1 l_2 l} \begin{pmatrix} l_1 & l_2 & l' \\ x & y & -(x+y) \end{pmatrix} \begin{pmatrix} l_1 & l_2 & l' \\ m_1 & m_2 & -m' \end{pmatrix} \int [_{-(x+y)}Y_{l' m'}^*] Y_{l_a m_a} [_{x+y}Y_{lm}^*] \\ &= \sum_{l_i m_i} (-1)^{l+l'} \sum_{l_a m_a} \mathcal{X}_{l_1 m_1} \mathcal{Y}_{l_2 m_2} w_{l_a m_a} I_{l_1 l_2 l'} I_{l' l_a l} \begin{pmatrix} l_1 & l_2 & l' \\ x & y & -(x+y) \end{pmatrix} \begin{pmatrix} l_1 & l_2 & l' \\ m_1 & m_2 & -m' \end{pmatrix} \\ &\quad \times \begin{pmatrix} l' & l_a & l \\ (x+y) & 0 & -(x+y) \end{pmatrix} \begin{pmatrix} l' & l_a & l \\ m' & m_a & -m \end{pmatrix}. \end{aligned} \quad (10)$$

In simplifying the relations derived in this section, we have used the relationship equations (34) and (35). We have also used the fact that $_{s}Y_{lm}^* = (-1)^{m+s} Y_{l,-m}$, where $*$ denotes the complex conjugate. Similarly, we can express the pseudo-harmonics of the field $\mathcal{Z}(\hat{\Omega})$ observed with the same mask in terms of its all-sky harmonics:

$$\begin{aligned} [\mathcal{Z}(\hat{\Omega})w(\hat{\Omega})]_{lm} &= \int d\hat{\Omega} [\mathcal{Z}(\hat{\Omega})w(\hat{\Omega})] [_{z}Y_{lm}^*] = \sum_{l_i m_i} \mathcal{Z}_{l_3 m_3} w_{l_b m_b} \int [_{z}Y_{l_3 m_3}(\hat{\Omega})][_{l_b m_b}Y_{lm}^*] d\hat{\Omega} \\ &= \sum_{l_3 m_3} \sum_{l_b m_b} \mathcal{Z}_{l_3 m_3} w_{l_b m_b} I_{l_3 l_b l} \begin{pmatrix} l_3 & l_b & l \\ z & y & -z \end{pmatrix} \begin{pmatrix} l_3 & l_b & l \\ m_3 & m_b & -m \end{pmatrix}. \end{aligned} \quad (11)$$

The harmonics of the composite field $[\mathcal{X}(\hat{\Omega})\mathcal{Y}(\hat{\Omega})]$, when constructed on a partial sky, are also functions of the harmonics of the mask used, w_{lm} . The simplest example of a mask would be $w = 1$ within the observed part of the sky and $w = 0$ outside. For a more complicated mask, the harmonics w_{lm} are constructed out of spherical harmonics transforms. We also need to apply the mask to the third field, which we will be using in our construction of the power spectrum related to the bispectrum (which we sometimes refer to as the skew spectrum) associated with these three fields. We will take the masks in each case to be the same, but the results could be very easily generalized for two

different masks. The *pseudo*-power spectrum is constructed from the masked harmonics of the relevant fields in the form of a cross-correlation power spectrum:

$$\tilde{C}_l^{\mathcal{X}\mathcal{Y},\mathcal{Z}} = \frac{1}{2l+1} \sum_{m=-l}^l [\mathcal{X}(\hat{\Omega})\mathcal{Y}(\hat{\Omega})w(\hat{\Omega})]_{lm} [\mathcal{Z}(\hat{\Omega})w(\hat{\Omega})]_{lm}^*. \quad (12)$$

The pseudo-power spectrum \tilde{C}_l is thus a linear combination of the modes of its all-sky counterpart C_l . In this sense, masking introduces a coupling of modes of various orders, which is absent in the case of all-sky coverage. The matrix $M_{ll'}$ encodes the information regarding the mode–mode coupling and depends on the power spectrum of the mask w_l . For surveys with partial sky coverage, the matrix is not invertible, which signifies the loss of information due to masking. Therefore, binning of the pseudo-skew spectrum or any higher order version based on, for example, kurtosis, may be necessary before it can be inverted, which leads to the recovery of an (unbiased) binned spectrum:

$$\tilde{C}_l^{\mathcal{X}\mathcal{Y},\mathcal{Z}} = \sum_{l'} M_{ll'}^{\mathcal{X}\mathcal{Y},\mathcal{Z}} C_{l'}^{\mathcal{X}\mathcal{Y},\mathcal{Z}}. \quad (13)$$

The all-sky power spectrum $C_l^{\mathcal{X}\mathcal{Y},\mathcal{Z}}$ can be recovered by inverting the equation related to the accompanying bispectrum by equation (7) discussed above. The mode–mode coupling matrix depends not only on the power spectrum $|w_l|$ of the mask, but also on the spin associated with the various fields, which are being probed in the construction of skew spectra:

$$M_{ll'}^{\mathcal{X}\mathcal{Y},\mathcal{Z}} = \frac{1}{4\pi} \sum_{l_a} (2l'+1)(2l_a+1) \begin{pmatrix} l & l_a & l' \\ x+y & 0 & -(x+y) \end{pmatrix} \begin{pmatrix} l & l_a & l' \\ z & 0 & -z \end{pmatrix} |w_{l_a}|^2. \quad (14)$$

This expression reduces to that of the temperature bispectrum, if we set all the spins to be zero, that is, $x = y = z = 0$, in which case the coupling of various modes due to partial sky coverage only depends on the power spectrum of the mask. In case of temperature-only (spin-0) analysis, we have seen that the mode–mode coupling matrix does not depend on the order of the statistics. The *skew spectrum* or the power spectrum related to bispectrum, as well as its higher order counterparts, such as the power spectrum related to trispectrum, can all have the same mode–mode coupling matrix in the presence of partial sky coverage. However, this is not the case for power spectra related to the polarization multispectra; that depends on the spin of various fields used to construct the bispectrum. It is customary to define a single number associated with each of these bispectra. The *skewness* is a weighted sum of the power spectrum related to the bispectrum $S_3^{\mathcal{X}\mathcal{Y},\mathcal{Z}} = \sum_l (2l+1) C_l^{\mathcal{X}\mathcal{Y},\mathcal{Z}}$.

We list the specific cases of interest below. The relations between the bispectra and the associated power spectra generalize cases previously obtained, where only the temperature bispectrum was considered (Cooray 2001):

$$C_l^{TT,E} = \sum_{l_1 l_2} B_{l_1 l_2 l}^{TTE} \sqrt{\frac{(2l_1+1)(2l_2+1)}{4\pi(2l+1)}} \begin{pmatrix} l_1 & l_2 & l \\ 0 & 0 & 0 \end{pmatrix} \quad (15)$$

$$M_{ll'}^{00,2} = \frac{1}{4\pi} \sum_{l_a} (2l'+1)(2l_a+1) \begin{pmatrix} l & l_a & l' \\ 0 & 0 & 0 \end{pmatrix} \begin{pmatrix} l & l_a & l' \\ 2 & 0 & -2 \end{pmatrix} |w_{l_a}|^2. \quad (16)$$

Next, we can express the power spectrum $C_l^{TE,E}$ probing the mixed bispectrum $B_{l_1 l_2 l}^{TEE}$ by the following relations:

$$C_l^{TE,E} = \sum_{l_1 l_2} B_{l_1 l_2 l}^{TEE} \sqrt{\frac{(2l_1+1)(2l_2+1)}{4\pi(2l+1)}} \begin{pmatrix} l_1 & l_2 & l \\ 2 & 0 & -2 \end{pmatrix}, \quad (17)$$

$$M_{ll'}^{02,2} = \frac{1}{4\pi} \sum_{l_a} (2l'+1)(2l_a+1) \begin{pmatrix} l & l_a & l' \\ 2 & 0 & -2 \end{pmatrix} \begin{pmatrix} l & l_a & l' \\ 2 & 0 & -2 \end{pmatrix} |w_{l_a}|^2. \quad (18)$$

Similarly, for the case $C_l^{EE,E}$, which probes the bispectrum $B_{l_1 l_2 l}^{EEE}$, we have the following expressions:

$$C_l^{EE,E} = \sum_{l_1 l_2} B_{l_1 l_2 l}^{EEE} \sqrt{\frac{(2l_1+1)(2l_2+1)}{4\pi(2l+1)}} \begin{pmatrix} l_1 & l_2 & l \\ 4 & 0 & -4 \end{pmatrix}, \quad (19)$$

$$M_{ll'}^{22,2} = \frac{1}{4\pi} \sum_{l_a} (2l'+1)(2l_a+1) \begin{pmatrix} l & l_a & l' \\ 4 & 0 & -4 \end{pmatrix} \begin{pmatrix} l & l_a & l' \\ 2 & 0 & -2 \end{pmatrix} |w_{l_a}|^2. \quad (20)$$

Other power spectra, such as $C_l^{EE,T}$ and those involving B-mode polarization, can be expressed in terms of the underlying bispectrum in a very similar manner. It is likely that future high-sensitivity experiments can probe these power spectra individually. As these are unbiased estimators, they can also be useful in testing simulation pipelines involving a large number of MC realizations, which are routinely used for standardization and characterization of data-analysis pipelines. The inversion of the coupling matrix $M_{ll'}$ can require binning, in which case the relevant binned coupling matrix $M_{bb'}$ in the case of small-sky coverage (such as ground-based and balloon-borne) surveys will lead to recovery of binned power spectra C_{lb} . The flat-sky analogues of these results can be useful in other cosmological studies, including weak-lensing observations, involving spin-2 fields (mapping out the shear or γ on the surface of the sky) that cover a small fraction of the sky. We plan to present results of such an analysis elsewhere (Munshi et al., in preparation).

2.2 The power spectrum associated with the trispectrum

The bispectrum represents the lowest-order deviation from Gaussianity; the next highest order is the trispectrum. There are many reasons for wanting to go beyond the lowest-order description. Many studies relating to secondary anisotropies have shown that ongoing surveys, such as *Planck*, can provide information about non-Gaussianity beyond the lowest order. These include the mode coupling of CMB due to weak lensing of CMB as well as the other secondary effects, such as thermal Sunyaev–Zeldovich and kinetic Sunyaev–Zeldovich effects (Cooray & Hu 2000; Munshi et al. 1995; Spergel et al. 1999a,b). With the recent (claimed) detection of primordial non-Gaussianity in the CMB, there has also been a renewed interest in detection of primordial non-Gaussianity beyond the lowest order with reasonable S/N. Such studies will constrain the parameters g_{NL} and f_{NL} independently. The S/N for such constraints is weaker than those achieved using a bispectrum, but with anticipated future increases in sensitivity of ongoing as well as future planned surveys, such studies will play an important role in future. Future 21-cm surveys can also provide valuable information about the trispectrum (Cooray, Li & Melchiorri 2008). A recent study by Munshi et al. (2009) constructed an estimator for a trispectrum, which can work with temperature data and which is optimized to detect primordial non-Gaussianity. This statistic was also applied to *WMAP* 5-yr data in Smidt et al. (2010) to provide the first constraints on τ_{NL} and g_{NL} , the third-order corrections to primordial perturbations in non-Gaussian models. We generalize and extend these works here to include both temperature and polarization data for an independent or joint estimate of such quantities.

2.2.1 The two-to-two power spectrum

In constructing the power spectrum related to the trispectrum, we start with two fields \mathcal{U} and \mathcal{V} , respectively, on the surface of the sphere. As before, we can take specific examples, where these fields are either P_{\pm} or δT . We will keep the analysis generic here, but will consider more specific examples later on. The spins associated with various fields are denoted by lower-case symbols, that is, u and v . The product field now can be expanded in terms of the spin harmonics of spin $u + v$, as was done in equation (6). Similarly, decomposing the other set of product fields, we obtain $[\mathcal{W}(\hat{\Omega})\mathcal{X}(\hat{\Omega})]_{lm}$. We next construct the power spectrum associated with the trispectrum from these harmonics:

$$C_l^{\mathcal{UV},\mathcal{WX}} = \frac{1}{2l+1} \sum_{m=-l}^l [\mathcal{U}(\hat{\Omega})\mathcal{V}(\hat{\Omega})]_{lm} [\mathcal{W}(\hat{\Omega})\mathcal{X}(\hat{\Omega})]_{lm}^*. \quad (21)$$

This particular type of power spectra associated with trispectra has been studied extensively in the literature in the context of CMB studies (see e.g. Cooray & Kesden 2003). It is one of the two degenerate power spectra associated with a trispectrum. After going through very similar algebra outlined in the previous section, we can express $C_l^{\mathcal{UV},\mathcal{WX}}$ in terms of the relevant trispectra, which it is probing. The resulting expression, in the absence of any mask, takes the following form:

$$C_l^{\mathcal{UV},\mathcal{WX}} = \sum_{l_1, l_2, l_3, l_4} T_{W_{l_3} X_{l_4}}^{U_{l_1} V_{l_2}}(l) \begin{pmatrix} l_1 & l_2 & l \\ u & v & -(u+v) \end{pmatrix} \begin{pmatrix} l_3 & l_4 & l \\ x & y & -(x+y) \end{pmatrix} \sqrt{\frac{(2l_1+1)(2l_2+1)}{(2l+1)}} \sqrt{\frac{(2l_3+1)(2l_4+1)}{(2l+1)}},$$

$$\mathcal{U}, \mathcal{V}, \mathcal{W}, \mathcal{X} \in P_{\pm}, \delta T; \quad (22)$$

$$\langle \mathcal{U}_{l_1 m_1} \mathcal{V}_{l_2 m_2} \mathcal{W}_{l_3 m_3} \mathcal{X}_{l_4 m_4} \rangle_c = \sum_{LM} (-1)^M \begin{pmatrix} l_1 & l_2 & L \\ m_1 & m_2 & -M \end{pmatrix} \begin{pmatrix} l_3 & l_4 & L \\ m_3 & m_4 & M \end{pmatrix} T_{W_{l_3} X_{l_4}}^{U_{l_1} V_{l_2}}(L) \quad (23)$$

In the presence of a completely general mask $w(\hat{\Omega})$, the PCLs will have to be modified. This involves computing the spherical harmonics of the masked field $\mathcal{U}(\hat{\Omega})\mathcal{V}(\hat{\Omega})w(\hat{\Omega})$ and cross-correlating it with the harmonics of $\mathcal{W}(\hat{\Omega})\mathcal{X}(\hat{\Omega})w(\hat{\Omega})$:

$$\tilde{C}_l^{\mathcal{UV},\mathcal{WX}} = \frac{1}{2l+1} \sum_{m=-l}^l [\mathcal{U}\mathcal{V}]_{lm} [\mathcal{W}\mathcal{X}w]_{lm}^*; \quad w_l = \frac{1}{2l+1} \sum_{m=-l}^l w_{lm} w_{lm}^*. \quad (24)$$

Again, the resulting PCLs are linear combinations of their all-sky counterparts. The mixing matrix, which encodes information about the mode mixing, will depend on the power spectrum of the mask as well as the spins of all four associated fields. The mixing matrix, $M_{ll'}$, expressed in terms of the Wigner-3j symbols takes the following form:

$$M_{ll'}^{uv,xy} = \frac{1}{4\pi} \sum_{l_a} (2l'+1)(2l_a+1) \begin{pmatrix} l & l_a & l' \\ u+v & 0 & -(u+v) \end{pmatrix} \begin{pmatrix} l & l_a & l' \\ x+y & 0 & -(x+y) \end{pmatrix} |w_{l_a}|^2; \quad u, v, x, y \in \pm 2, 0. \quad (25)$$

The PCLs expressed as a linear combination of all-sky power spectra can now be expressed using the following relationship:

$$\tilde{C}_l^{\mathcal{UV},\mathcal{WX}} = \sum_{l'} M_{ll'}^{uvwx} C_{l'}^{\mathcal{UV},\mathcal{WX}}. \quad (26)$$

For nearly-complete sky surveys, and with proper binning, the mixing matrix $M_{ll'}$ can be made invertible. This provides a unique way to estimate all-sky $C_{l'}^{UVWX}$ and extract the information it contains about the trispectra. For a given theoretical prediction, the all-sky power spectra $C_{l'}^{UVWX}$ can be analytically computed. Knowing the detailed model of an experimental mask then allows us to compute the observed \tilde{C}_l^{UVWX} accurately. The results presented here generalize those obtained in Munshi et al. (2009) for the case of polarization studies.

These results assume generic field variables $\mathcal{X}(\hat{\Omega})$, $\mathcal{Y}(\hat{\Omega})$, which can have arbitrary spin associated to them. We next specify certain specific cases, where we identify three of the fields \mathcal{X} , \mathcal{Y} , $\mathcal{Z} = \delta_T$ and $\mathcal{Z} = P_+ = E$. The other combinations can also be obtained in a similar manner:

$$C_l^{TT,TE} = \sum_{l_1, l_2, l_3, l_4} T_{T_{l_3} E_{l_4}}^{T_{l_1} T_{l_2}}(l) \begin{pmatrix} l_1 & l_2 & l \\ 0 & 0 & 0 \end{pmatrix} \begin{pmatrix} l_3 & l_4 & l \\ 2 & 0 & -2 \end{pmatrix} \sqrt{\frac{(2l_1+1)(2l_2+1)}{(2l+1)}} \sqrt{\frac{(2l_3+1)(2l_4+1)}{(2l+1)}}; \quad (27)$$

$$M_{ll'}^{00,02} = \frac{1}{4\pi} \sum_{l_a} (2l'+1)(2l_a+1) \begin{pmatrix} l & l_a & l' \\ 0 & 0 & 0 \end{pmatrix} \begin{pmatrix} l & l_a & l' \\ 2 & 0 & -2 \end{pmatrix} |w_{l_a}|^2; \quad (28)$$

Other estimators for mixed trispectra, involving different combinations of E polarization and temperature anisotropy δ_T , can be derived in a similar manner and can provide independent information of corresponding trispectra. As before, we have ignored the presence of B-type polarization in our analysis. The presence of a non-zero B mode can be dealt with very easily in our framework, but the resulting expressions will be more complicated.

2.2.2 The three-to-one power spectrum

The number of power spectra that can be associated with a given multispectrum depends on the number of different ways the order of the multispectrum can be decomposed into a pair of integers. The bispectrum being of the order of 3 can be decomposed uniquely, $3 = 2 + 1$, and has only one associated power spectrum. On the other hand, the order of the trispectrum can be decomposed in two different ways, that is, $4 = 3 + 1 = 2 + 2$. Hence, the trispectrum of a specific type generates a pair of two different power spectra associated with it (see e.g. Munshi et al. 2009 for more details). The results presented here are generalizations for the case of non-zero spins.

The other power spectrum associated with the trispectrum is constructed by cross-correlating the product of three different fields $[\mathcal{UVW}]$ with the remaining field $[\mathcal{X}]$. The cross-correlation power spectrum in terms of the multipoles is given by the following expression:

$$[\mathcal{UVW}]_{lm} = \int [\mathcal{U}(\hat{\Omega})\mathcal{V}(\hat{\Omega})\mathcal{X}(\hat{\Omega})] [{}_{u+v+w}Y_{lm}(\hat{\Omega})^*] d\hat{\Omega}; \quad [\mathcal{Z}]_{lm} = \int [\mathcal{X}(\hat{\Omega})] [{}_zY_{lm}(\hat{\Omega})^*] d\hat{\Omega}; \quad C_l^{\mathcal{UVW},\mathcal{X}} = \frac{1}{2l+1} \sum_{m=-l}^l [\mathcal{UVW}]_{lm} [\mathcal{X}]_{lm}^*. \quad (29)$$

By repeated use of the expressions, equation (34) or, equivalently, equation (35), to simplify the harmonics of the product field in terms of the individual harmonics, we can express the all-sky result in the following form:

$$C_l^{\mathcal{UVW},\mathcal{X}} = \sum_{l_1, l_2, l_3, L} T_{\mathcal{W}_{l_3} \mathcal{X}_{l_1}}^{\mathcal{U}_{l_1} \mathcal{V}_{l_2}}(L) \begin{pmatrix} l_1 & l_2 & L \\ u & v & -(u+v) \end{pmatrix} \begin{pmatrix} L & l_3 & l' \\ (u+v) & w & -(u+v+w) \end{pmatrix} \sqrt{\frac{(2l_1+1)(2l_2+1)}{(2L+1)}} \sqrt{\frac{(2L+1)(2l_3+1)}{(2l+1)}}. \quad (30)$$

In the case of partial sky coverage with a generic mask $w(\hat{\Omega})$, the relevant expression for the PCLs will as usual involve the harmonic transform of the mask:

$$[\mathcal{UVW}w]_{lm} = \int [\mathcal{U}(\hat{\Omega})\mathcal{V}(\hat{\Omega})\mathcal{W}(\hat{\Omega})w(\hat{\Omega})] [{}_{u+v+w}Y_{lm}^*(\hat{\Omega})] d\hat{\Omega}; \quad [\mathcal{X}w]_{lm} = \int [\mathcal{X}(\hat{\Omega})w(\hat{\Omega})] [{}_zY_{lm}^*(\hat{\Omega})] d\hat{\Omega}; \quad \tilde{C}_l^{\mathcal{UVW},\mathcal{X}} = M_{ll'} C_{l'}^{\mathcal{UVW},\mathcal{X}} \quad (31)$$

The mixing matrix has the following expression in terms of various spins involved and the power spectra of the mask introduced above. Note that the mixing matrix is of different form compared to what we obtained for two-to-one power spectra. This is related to how various fields with different spins were combined to construct the two estimators. In the case of a temperature trispectrum (spin 0), the two mixing matrices take the same form:

$$M_{ll'}^{uvw,x} = \frac{1}{4\pi} \sum_{l_a} (2l'+1)(2l_a+1) \begin{pmatrix} l & l_a & l' \\ (u+v+w) & 0 & -(u+v+w) \end{pmatrix} \begin{pmatrix} l & l_a & l' \\ x & 0 & -x \end{pmatrix} |w_{l_a}|^2. \quad (32)$$

The expressions derived here apply to a general mask and to correlated Gaussian instrument noise; any non-Gaussianity from the noise will have to be allowed for. These calculations lead to optimal estimators, but the weights required depend on the precise model of non-Gaussianity being assumed. We present the models for primordial non-Gaussianity in the next section and use them to construct optimal estimator in our later discussions.

For a specific example, we choose $\mathcal{U} = \mathcal{V} = \mathcal{W} = \delta_T$ and $\mathcal{X} = \mathcal{E}$. In this case, the three-to-one estimator takes the following form:

$$C_l^{TTT,E} = \sum_{l_1, l_2, l_3, L} T_{T_{l_3} E_{l_1}}^{T_{l_1} T_{l_2}}(L) \begin{pmatrix} l_1 & l_2 & L \\ 0 & 0 & 0 \end{pmatrix} \begin{pmatrix} L & l_3 & l \\ 0 & 0 & 0 \end{pmatrix} \sqrt{\frac{(2l_1+1)(2l_2+1)}{(2L+1)}} \sqrt{\frac{(2L+1)(2l_3+1)}{(2l+1)}}; \quad (33)$$

$$M_{ll'}^{000,2} = \frac{1}{4\pi} \sum_{l_a} (2l'+1)(2l_a+1) \begin{pmatrix} l & l_a & l' \\ 0 & 0 & 0 \end{pmatrix} \begin{pmatrix} l & l_a & l' \\ 2 & 0 & -2 \end{pmatrix} |w_{l_a}|^2.$$

The bispectrum is defined through a triangular configuration in the multipole space, the trispectrum with a quadrilateral (which can be decomposed into two constituent triangles). The Wigner-3j symbols enforce these constraints at various levels for a bispectrum and trispectrum.

The two-to-one power spectrum or skew spectrum introduced in previous sections essentially sums over all possible configurations of the triangle obtained by keeping one of its sides fixed. In an analogous manner, the two probes of a trispectrum introduced here are linked with two different configurations in the harmonic domain. The two-to-two power spectrum keeps the diagonal of the quadrilateral fixed, whereas the three-to-one power spectrum keeps one of the sides fixed, while summing over all other possible configurations.

It is possible to introduce a window optimized to search selectively for information for a specific configuration for either the bispectrum or the trispectrum. However, such analysis, which introduces mode–mode coupling, cannot be generalized to the arbitrary partial sky coverage, as there is already a coupling of modes because of non-uniform coverage of the sky.

Unlike the bispectrum, the trispectrum has a non-vanishing contribution from the Gaussian component of a CMB map (in the same way that, while the third moment of a univariate Gaussian about the mean is zero, the corresponding fourth-order moment is not). The Gaussian contribution represents the unconnected component of the total trispectrum, which needs to be subtracted out. This can be done by generating MC maps using an identical mask. The resulting Gaussian part of the spectra can then be subtracted from the estimates from the real data. The procedure is similar to the analysis of temperature-only data (for more details see Munshi et al. 2009). Noise (assumed Gaussian) can also be subtracted out following a similar procedure. The treatment requires a hit-count map from a realistic scanning strategy, for non-uniform distribution of noise, from where the variance of noise distribution in each pixel can be constructed.

To derive and simplify the above expressions, we have used the following results related to the overlap integral involving three spin harmonics, which generalizes the well-known *Gaunt Integrals* involving spin-0 spherical harmonics:

$$\int_s Y_{lm}(\hat{\Omega})_s Y_{l'm'}(\hat{\Omega})_{s'} Y_{l''m''}(\hat{\Omega})_{s''} d\hat{\Omega} = \sqrt{\frac{(2l+1)(2l'+1)(2l''+1)}{4\pi}} \begin{pmatrix} l & l' & l'' \\ m & m' & m'' \end{pmatrix} \begin{pmatrix} l & l' & l'' \\ -s & -s' & -s'' \end{pmatrix}. \quad (34)$$

The above result can be cast in the following form, which is useful for expressing an integral of more than three spin spherical harmonics in terms of Wigner-3j symbols:

$${}_s Y_{lm}(\hat{\Omega})_s {}_{s'} Y_{l'm'}(\hat{\Omega})_{s'} = \sum_{LSM} {}_s Y_{LM}^* \sqrt{\frac{(2L+1)(2l'+1)(2l''+1)}{4\pi}} \begin{pmatrix} L & l' & l'' \\ M & m' & m'' \end{pmatrix} \begin{pmatrix} L & l' & l'' \\ -S & -s' & -s'' \end{pmatrix}. \quad (35)$$

The Wigner-3j symbols satisfy an orthogonality relationship which can be written as

$$\sum_{m_1 m_2} \begin{pmatrix} l_1 & l_2 & l_a \\ m_1 & m_2 & m_a \end{pmatrix} \begin{pmatrix} l_1 & l_2 & l_b \\ m_1 & m_2 & m_b \end{pmatrix} = \frac{\delta_{l_a l_b} \delta_{m_a m_b}}{2l_a + 1}. \quad (36)$$

In the remainder of this paper, we will generalize the estimators by including inverse-variance weighting. We will first show how to include the effect of noise and mask by using MC simulations. Next, we will consider the exact inverse-variance weighting, where the inverse-covariance matrix incorporates the effect of noise and mask.

Note that incorporating a non-zero B-type (magnetic) polarization is possible in our formalism presented above by conceptually trivial extension. We have only taken into account E-type (electric) polarization to keep the derivations simple as E modes are assumed to dominate the presence of B-mode polarization.

3 THE BISPECTRUM AND TRISPECTRUM WITH PRIMORDIAL NON-GAUSSIANITY

The optimization techniques that we will introduce in this section follow the discussion in Munshi & Heavens (2010) and Munshi et al. (2009). The optimization procedure depends on construction of three-dimensional fields from the harmonic components of the temperature fields a_{lm} with suitable weighting with respective functions (α, β, μ) , which describes primordial non-Gaussianity (Yadav, Komatsu & Wandelt 2007). These weights make the estimators act in an optimal way and the matched filtering technique adopted ensures that the response to the observed non-Gaussianity is maximum, when it matches with the target primordial non-Gaussianity corresponding to the weights.

In the linear regime, the curvature perturbations, which generate the fluctuations in the CMB sky, are written as

$$a_{lm}^{\mathcal{X}} = 4\pi(-i)^l \int \frac{d^3 k}{(2\pi)^3} \Phi(\mathbf{k}) \Delta_l^{\mathcal{X}}(k) Y_{lm}(\hat{k}); \quad \mathcal{X} \in T, E. \quad (37)$$

We will need the following functions to construct the harmonic space trispectrum as well as to generate weights for the construction of optimal estimators:

$$\alpha_l^{\mathcal{X}}(r) = \frac{2}{\pi} \int_0^\infty k^2 dk \Delta_l^{\mathcal{X}}(k) j_l(kr); \quad \beta_l^{\mathcal{X}}(r) = \frac{2}{\pi} \int_0^\infty k^2 dk P_\phi(k) \Delta_l^{\mathcal{X}}(k) j_l(kr); \quad \mu_l^{\mathcal{X}}(r) = \frac{2}{\pi} \int_0^\infty k^2 dk \Delta_l^{\mathcal{X}}(k) j_l(kr). \quad (38)$$

For a more complete description of the method for extracting the trispectrum from a given inflationary model, see Hu (2000) and Hu & Okamoto (2002). In the limit of low multipoles, where the perturbations are mainly dominated by the Sachs–Wolfe effect, the transfer functions $\Delta_l(k)$ take a rather simple form $\Delta_l(k) = j_l(kr_*)/3$, where $r_* = (\eta_0 - \eta_{\text{dec}})$ denotes the time elapsed between cosmic recombination and the present epoch. In general, the transfer function needs to be computed numerically. The *local* model for the primordial bispectrum and trispectrum can be constructed by going beyond linear theory in the expansion of $\Phi(x)$. Additional parameters f_{NL} and g_{NL} are introduced, which need to be estimated from observation. As discussed in the introduction, g_{NL} can be linked to r , the *scalar-to-tensor ratio* in a specific inflationary model and hence expected to be small:

$$\Phi(\mathbf{x}) = \Phi_L(\mathbf{x}) + f_{\text{NL}} (\Phi_L^2(\mathbf{x}) - \langle \Phi_L^2(\mathbf{x}) \rangle) + g_{\text{NL}} \Phi_L^3(\mathbf{x}) + h_{\text{NL}} (\Phi_L^4(\mathbf{x}) - 3 \langle \Phi_L^2(\mathbf{x}) \rangle^2) + \dots \quad (39)$$

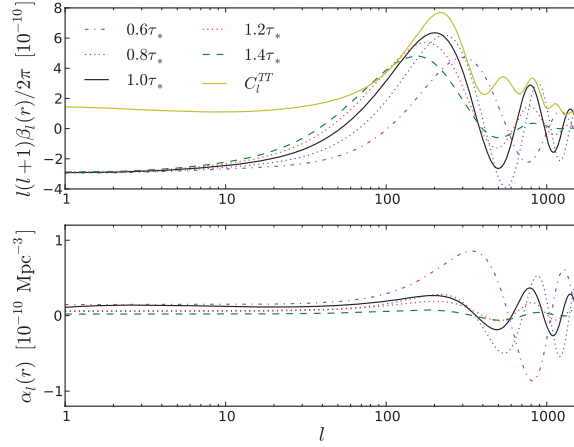


Figure 1. $\alpha(r)$ (lower panel) and $\beta(r)$ (upper panel) for the temperature are plotted as a function of l . Plots are based on WMAP7 parameters (Larson et al. 2010).

We will only consider the local model of primordial non-Gaussianity in this paper and only adiabatic initial perturbations. More complicated cases of primordial non-Gaussianity will be dealt with elsewhere. In terms of the inflationary potential, $V(\phi)$, associated with a scalar potential, ϕ , one can express these constants as (Hu 2000):

$$f_{\text{NL}} = -\frac{5}{6} \frac{1}{8\pi G} \frac{\partial^2 \ln V(\phi)}{\partial \phi^2}; \quad g_{\text{NL}} = \frac{25}{54} \frac{1}{(8\pi G)^2} \left[2 \left(\frac{\partial^2 \ln V(\phi)}{\partial \phi^2} \right)^2 - \left(\frac{\partial^3 \ln V(\phi)}{\partial \phi^3} \right) \left(\frac{\partial \ln V(\phi)}{\partial \phi} \right) \right]. \quad (40)$$

There are two contributions to the primordial non-Gaussianity. The first part is parametrized by f_{NL} and the second contribution is proportional to a new parameter, which appears at fourth order, denoted by g_{NL} . From theoretical considerations in generic models of inflation, one would expect $g_{\text{NL}} \leq r/50$ (Seery, Lidsey & Sloth 2007). Following Hu (2000), we can expand the above expression in Fourier space to write

$$\Phi_2(k) = \int \frac{d^3 k_1}{(2\pi)^3} \Phi_L(k + k_1) \Phi_L^*(k_1) - (2\pi)^3 \delta_D(k) \int \frac{d^3 k_1}{(2\pi)^3} P_{\Phi\Phi}(k_1); \quad \Phi_3(k) = \int \frac{d^3 k}{(2\pi)^3} \Phi_L(k_1) \Phi_L(k_2) \Phi_L^*(k_1). \quad (41)$$

The resulting trispectrum T_Φ for the potential Φ associated with these perturbations can be expressed as

$$T_\Phi(k_1, k_2, k_3, k_4) \equiv \langle \Phi(k_1) \Phi(k_2) \Phi(k_3) \Phi(k_4) \rangle_c = \int \frac{d^3 K}{(2\pi)^3} \delta_D(k_1 + k_2 - K) \delta_D(k_3 + k_4 + K) \mathcal{T}_\Phi(k_1, k_2, k_3, k_4, K), \quad (42)$$

where the reduced trispectrum $\mathcal{T}(k_1, k_2, k_3, k_4, K)$ can be decomposed into two distinct contributions

$$\mathcal{T}_\Phi^{(2)}(k_1, k_2, k_3, k_4, K) = 4f_{\text{NL}}^2 P_\Phi(K) P_\Phi(k_1) P_\Phi(k_3); \quad \mathcal{T}_\Phi^{(3)}(k_1, k_2, k_3, k_4, K) = g_{\text{NL}} \{ P_\Phi(K) P_\Phi(k_1) P_\Phi(k_3) + P_\Phi(K) P_\Phi(k_1) P_\Phi(k_3) \}. \quad (43)$$

The resulting mixed trispectrum, involving temperature and E-type polarization, now can be written as

$$T_{\mathcal{W}_{l_3}^{\mathcal{U}_{l_1} \mathcal{V}_{l_2}} \mathcal{X}_{l_4}}(L) = 4f_{\text{NL}}^2 I_{l_1 l_2 L} I_{l_3 l_4 L} \int r_1^2 dr_1 r_2^2 dr_2 F_L(r_1, r_2) \alpha_{l_1}^{\mathcal{U}}(r_1) \beta_{l_2}^{\mathcal{V}}(r_1) \alpha_{l_3}^{\mathcal{W}}(r_2) \beta_{l_4}^{\mathcal{X}}(r_2) \\ + g_{\text{NL}} I_{l_1 l_2 L} I_{l_3 l_4 L} \int r^2 dr \beta_{l_2}^{\mathcal{V}}(r) \beta_{l_4}^{\mathcal{X}}(r) [\mu_{l_1}^{\mathcal{U}}(r) \beta_{l_3}^{\mathcal{W}}(r) + \mu_{l_3}^{\mathcal{W}}(r) \beta_{l_1}^{\mathcal{U}}(r)]. \quad (44)$$

For detailed descriptions of objects, such as α , β , μ and F_L , see Hu & Okamoto (2002), Hu (2000), Komatsu & Spergel (2001) and Kogo & Komatsu (2006). We plot $\alpha_l(v)$ and $\beta_l(v)$ for T and E in Fig. 1 and Fig. 2 respectively. The CMB bispectrum, which describes departures from Gaussianity at the lowest level, can be analysed in a similar fashion [see Munshi & Heavens (2010) for a detailed discussion and Smidt et al. (2009) for a measurement in data]. The corresponding expression is

$$B_{l_1 l_2 l_3}^{\mathcal{U}_{l_1} \mathcal{V}_{l_2} \mathcal{W}_{l_3}} = 2f_{\text{NL}} I_{l_1 l_2 l_3} \int r^2 dr [\alpha_{l_1}^{\mathcal{U}}(r) \beta_{l_2}^{\mathcal{V}}(r) \beta_{l_3}^{\mathcal{W}}(r) + \alpha_{l_2}^{\mathcal{V}}(r) \beta_{l_3}^{\mathcal{W}}(r) \beta_{l_1}^{\mathcal{U}}(r) + \alpha_{l_3}^{\mathcal{W}}(r) \beta_{l_1}^{\mathcal{U}}(r) \beta_{l_2}^{\mathcal{V}}(r)]. \quad (45)$$

The extension to orders beyond those presented here involves higher order Taylor coefficients and may not be practically useful as detector noise and the cosmic variance may prohibit any reasonable S/N. Numerical evaluations of the functions α , β and μ can be performed by using the publicly available Boltzmann solvers, such as CAMB⁴ or CMBFAST.⁵

A Gaussian fluctuation field has zero bispectrum. However, even a Gaussian map will have non-zero trispectrum; this corresponds to the unconnected part of the trispectrum. Its contribution can be expressed in terms of the cross-power spectra associated with contributing fields:

$$G_{\mathcal{W}_{l_3}^{\mathcal{U}_{l_1} \mathcal{V}_{l_2}} \mathcal{X}_{l_4}}^{\mathcal{U}_{l_1} \mathcal{V}_{l_2}}(L) = (-1)^{(l_1+l_3)} \sqrt{(2l_1+1)(2l_3+1)} C_{l_1}^{\mathcal{U}} C_{l_3}^{\mathcal{W}} \delta_{l_1 l_2} \delta_{l_3 l_4} \delta_{L0} + (2L+1) [(-1)^{l_1+l_2+L} C_{l_1}^{\mathcal{U}} C_{l_2}^{\mathcal{V}} \delta_{l_1 l_3} \delta_{l_2 l_4} + C_{l_1}^{\mathcal{U}} C_{l_2}^{\mathcal{V}} \delta_{l_1 l_4} \delta_{l_2 l_3}] \quad (46)$$

⁴ <http://camb.info>

⁵ <http://www.cmbfast.org>

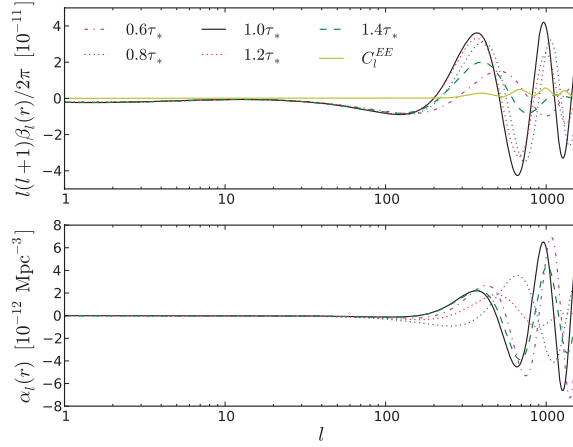


Figure 2. Same as the previous plot, but for E-type polarization.

In the case of Gaussian maps, the trispectrum can be expressed completely in terms of the relevant cross-power spectra $C_l^{\mathcal{U}\mathcal{V}}$ of corresponding fields \mathcal{U} and \mathcal{V} . The estimators designed in later sections estimate the combined skew or kurt spectra, and the Gaussian contributions are subtracted accordingly. The Gaussian maps that are used for MC estimates of bias and scatter are constructed to have the same power spectrum as the non-Gaussian maps being analysed.

4 PARTIAL SKY COVERAGE AND INHOMOGENEOUS NOISE

In this section, we consider the inverse-variance weighting of the data. We will consider the all-sky case first and then introduce the analytical results that can handle data in the presence of partial sky coverage as well as correlated Gaussian noise. The method developed here relies on MC simulations to model observational artefacts. These estimators use a weighted version of square temperature–temperature (or two-to-one) angular power spectra. In a manner similar to its simpler version introduced in the previous section, this power spectrum extracts information from the bispectrum as a function of length of one side of the triangle in harmonic space, while summing over all possible configurations given by the change of other two sides of the triangle.

4.1 Bispectrum-related power spectrum or skew spectrum

Following Komatsu et al. (2005), we first construct the three-dimensional fields $A(r, \hat{\Omega})$ and $B(r, \hat{\Omega})$ from the expansion coefficients of the observed CMB map, a_{lm} . The harmonics here, $A_{lm}(r)$ and $B_{lm}(r)$, are simply weighted spherical harmonics of the temperature field, a_{lm} , with weights constructed from the CMB power spectrum C_l and the functions $\alpha_l(r)$ and $\beta_l(r)$, respectively:

$$A^{\mathcal{U}}(r, \hat{\Omega}) \equiv \sum_{lm} Y_{lm}(\hat{\Omega}) A_{lm}^{\mathcal{U}}(r); \quad A_{lm}^{\mathcal{U}}(r) \equiv \alpha_l^{\mathcal{U}}(r) \sum_{\mathcal{U}'} \sum_{l'm'} [\mathbf{C}^{-1}]_{\mathcal{U}\mathcal{U}'} b_{l'} a_{l'm'}^{\mathcal{U}'} = \alpha_l^{\mathcal{U}} b_l \tilde{a}_{lm}^{\mathcal{U}}; \quad (47)$$

$$B^{\mathcal{U}}(r, \hat{\Omega}) \equiv \sum_{lm} Y_{lm}(\hat{\Omega}) B_{lm}^{\mathcal{U}}(r); \quad B_{lm}^{\mathcal{U}}(r) \equiv \beta_l^{\mathcal{U}}(r) \sum_{\mathcal{U}'} \sum_{l'm'} [\mathbf{C}^{-1}]_{\mathcal{U}\mathcal{U}'} b_{l'} a_{l'm'}^{\mathcal{U}'} = \beta_l^{\mathcal{U}} b_l \tilde{a}_{lm}^{\mathcal{U}}. \quad (48)$$

The function b_l represents beam smoothing, and from here onwards, we will absorb it into the harmonic transforms. The matrix \mathbf{C} depends on both temperature (T) and E-type polarization power spectra, C_l^{TT} and C_l^{EE} . The cross-correlation power spectrum is denoted by C_l^{TE} .

$$[\mathbf{C}]_l = \begin{pmatrix} C_l^{TT} & C_l^{TE} \\ C_l^{TE} & C_l^{EE} \end{pmatrix}; \quad [\mathbf{C}]_l^{-1} = \frac{1}{\mathcal{D}_l} \begin{pmatrix} -C_l^{EE} & C_l^{TE} \\ C_l^{TE} & -C_l^{TT} \end{pmatrix}; \quad \tilde{a}^{\mathcal{U}} = [\mathbf{C}]_{\mathcal{U}\mathcal{U}'}^{-1} a^{\mathcal{U}'} \quad (49)$$

The determinant \mathcal{D}_l introduced above is a function of the relevant three power spectra introduced above $\mathcal{D}_l = C_l^{TT} C_l^{EE} - (C_l^{TE})^2$ for joint (T, E) analysis. Using these definitions, Komatsu et al. (2005) defined the one-point mixed skewness involving the fields $A^i(r, \hat{\Omega})$ and $B^j(r, \hat{\Omega})$ ($i, j, k \in T, E$):

$$S^{A^{\mathcal{U}} B^{\mathcal{V}} B^{\mathcal{W}}} \equiv \int r^2 dr \int d\hat{\Omega} A^{\mathcal{U}}(r, \hat{\Omega}) B^{\mathcal{V}}(r, \hat{\Omega}) B^{\mathcal{W}}(r, \hat{\Omega}). \quad (50)$$

$S^{A^{\mathcal{U}} B^{\mathcal{V}} B^{\mathcal{W}}}$ can be used to estimate $f_{\text{NL}}^{\text{loc}}$, but such a radical compression of the data into a single number restricts the ability to estimate contamination of the estimator by other sources of non-Gaussianity. As a consequence, we construct a less-radical compression, to a function of l , which can be used to estimate $f_{\text{NL}}^{\text{loc}}$, but which can also be analysed for contamination by, for example, foregrounds. We do this by constructing the integrated cross-power spectrum of the maps $A^{\mathcal{U}}(r, \hat{\Omega})$ and $B^{\mathcal{V}}(r, \hat{\Omega}) B^{\mathcal{W}}(r, \hat{\Omega})$. Expanding B^2 in spherical harmonics gives

$$[B^{\mathcal{V}}(\hat{\Omega}, r) B^{\mathcal{W}}(\hat{\Omega}, r)]_{lm} \equiv \int d\hat{\Omega} B^{\mathcal{V}}(r, \hat{\Omega}) B^{\mathcal{W}}(r, \hat{\Omega}) Y_{lm}(\hat{\Omega}) = \sum_{l'm'} \sum_{l''m''} \beta_{l'}^{\mathcal{V}}(r) \beta_{l''}^{\mathcal{W}}(r) \begin{pmatrix} l & l' & l'' \\ m & m' & m'' \end{pmatrix} I_{ll''m''} \tilde{a}_{l'm'}^{\mathcal{V}} \tilde{a}_{l''m''}^{\mathcal{W}} \quad (51)$$

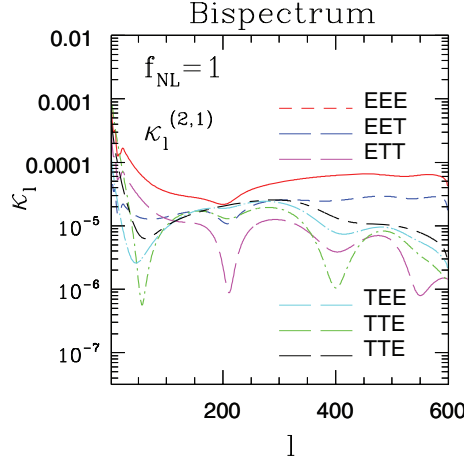


Figure 3. Various bispectrum-related power spectra $(2l+1)\kappa_l^{(2,1)}$ plotted as a function of angular scale l . We use $f_{\text{NL}} = 1$ for each of these plots. Plots are based on *WMAP7* (Larson et al. 2010) parameters equated out to $l_{\text{max}} = 500$.

and we define the cross-power spectrum $C_l^{A,B^2}(r)$ at a radial distance r as

$$C_l^{A^{\mathcal{U}}, B^{\mathcal{V}} B^{\mathcal{W}}}(r) = \frac{1}{2l+1} \sum_m \text{Real} \{ A_{lm}^{\mathcal{U}}(r) [B^{\mathcal{V}}(r) B^{\mathcal{W}}(r)]_{lm} \}. \quad (52)$$

Integrating over r , we get

$$C_l^{A^{\mathcal{U}}, B^{\mathcal{V}} B^{\mathcal{W}}} \equiv \int r^2 dr C_l^{A^{\mathcal{U}}, B^{\mathcal{V}} B^{\mathcal{W}}}(r). \quad (53)$$

This integrated cross-power spectrum of $B^2(r, \hat{\Omega})$ and $A(r, \hat{\Omega})$ carries information about the underlying bispectrum $B_{ll'l''}$, as follows:

$$\hat{C}_l^{A^{\mathcal{U}}, B^{\mathcal{V}} B^{\mathcal{W}}} = \frac{1}{2l+1} \sum_m \sum_{l'm'} \sum_{l''m''} I_{ll'l''} \begin{pmatrix} l & l' & l'' \\ m & m' & m'' \end{pmatrix} \int r^2 dr \{ \alpha_l^{\mathcal{U}}(r) \beta_{l'}^{\mathcal{V}}(r) \beta_{l''}^{\mathcal{W}}(r) \} \tilde{a}_{lm}^{\mathcal{U}} \tilde{a}_{l'm'}^{\mathcal{V}} \tilde{a}_{l''m''}^{\mathcal{W}}. \quad (54)$$

Similarly, we can construct the cross-power-spectrum of the product map $A^{\mathcal{U}} B^{\mathcal{V}}(r, \hat{\Omega})$ and $B^{\mathcal{W}}(r, \hat{\Omega})$, which we denote as $C_l^{A^{\mathcal{U}} B^{\mathcal{V}}, B^{\mathcal{W}}}$:

$$\hat{C}_l^{A^{\mathcal{U}} B^{\mathcal{V}}, B^{\mathcal{W}}} = \frac{1}{2l+1} \sum_m \sum_{l'm'} \sum_{l''m''} I_{ll'l''} \begin{pmatrix} l & l' & l'' \\ m & m' & m'' \end{pmatrix} \int r^2 dr \{ \beta_l^{\mathcal{W}}(r) \alpha_{l'}^{\mathcal{U}}(r) \beta_{l''}^{\mathcal{V}}(r) \} \tilde{a}_{lm}^{\mathcal{U}} \tilde{a}_{l'm'}^{\mathcal{V}} \tilde{a}_{l''m''}^{\mathcal{W}}. \quad (55)$$

Using these expressions, and the following relation, we can write this more compactly in terms of the estimated CMB bispectrum

$$\hat{B}_{ll'l''}^{\mathcal{U}\mathcal{V}\mathcal{W}} = \sum_{mm'm''} \begin{pmatrix} l & l' & l'' \\ m & m' & m'' \end{pmatrix} a_{lm}^{\mathcal{U}} a_{l'm'}^{\mathcal{V}} a_{l''m''}^{\mathcal{W}}, \quad (56)$$

from which we compute our new statistic, the *bispectrum-related power spectrum*, C_l^{loc} as

$$\hat{C}_l^{A^{\mathcal{U}} B^{\mathcal{V}} B^{\mathcal{W}}} \equiv \left(\hat{C}_l^{A^{\mathcal{U}}, B^{\mathcal{V}} B^{\mathcal{W}}} + \hat{C}_l^{A^{\mathcal{U}} B^{\mathcal{V}}, B^{\mathcal{W}}} + \hat{C}_l^{A^{\mathcal{U}} B^{\mathcal{W}}, B^{\mathcal{V}}} \right) = \frac{\hat{f}_{\text{NL}}^{\text{loc}}}{(2l+1)} \sum_{\mathcal{U}\mathcal{V}\mathcal{W}} \sum_{l'} \sum_{l''} \left\{ B_{ll'l''}^{\mathcal{U}\mathcal{V}\mathcal{W}} [\mathbf{C}^{-1}]_l^{\mathcal{U}\mathcal{U}'} [\mathbf{C}^{-1}]_{l'}^{\mathcal{V}\mathcal{V}'} [\mathbf{C}^{-1}]_{l''}^{\mathcal{W}\mathcal{W}'} B_{ll'l''}^{\mathcal{U}'\mathcal{V}'\mathcal{W}'} \right\}. \quad (57)$$

Clearly, in a joint analysis, the *pure skew spectrum*, such as $C_l^{T,TT}$ or $C_l^{E,EE}$, discussed in the previous section gets generalized to $C_l^{A^{\mathcal{U}}, B^{\mathcal{V}} B^{\mathcal{W}}}$, etc., and the construction of inverse-covariance weighted fields mixes temperature and E-type polarization (see Fig. 3). Hence, each of these estimators carries information from all possible types of mixed bispectra. If we combine various estimates into a unique power spectrum, then it compresses all available information for T and E-type polarization maps:

$$\hat{C}_l^{(2,1)} = \sum_{\mathcal{U}\mathcal{V}\mathcal{W}} \hat{C}_l^{A^{\mathcal{U}} B^{\mathcal{V}} B^{\mathcal{W}}}, \quad (58)$$

where $B_{ll'l''}^{\text{loc}}$ is the bispectrum for the local f_{NL} model, normalized to $f_{\text{NL}}^{\text{loc}} = 1$. We can now use standard statistical techniques to estimate $f_{\text{NL}}^{\text{loc}}$. Note that if we sum over all l values, then we recover the estimator S_{prim} of Komatsu et al. (2005), which is the cross-skewness of ABB :

$$\hat{S}_3^{A^{\mathcal{U}} B^{\mathcal{V}} B^{\mathcal{W}}} = \sum_l (2l+1) \left(\hat{C}_l^{A^{\mathcal{U}}, B^{\mathcal{V}} B^{\mathcal{W}}} + \hat{C}_l^{A^{\mathcal{U}} B^{\mathcal{V}}, B^{\mathcal{W}}} + \hat{C}_l^{A^{\mathcal{U}} B^{\mathcal{W}}, B^{\mathcal{V}}} \right). \quad (59)$$

If we sum over all possible triplets ijk , we can recover S_3 typically used in the literature and considered previously (Munshi & Heavens 2010):

$$\hat{S}_3 = \sum_{\mathcal{U}\mathcal{V}\mathcal{W}} \hat{S}_3^{A^{\mathcal{U}} B^{\mathcal{V}} B^{\mathcal{W}}}. \quad (60)$$

Though S_3 compresses all available information at the level of the bispectrum in temperature and polarization maps, it clearly also has less power to distinguish any effect of systematics. These can be studied in more detail, if we carry out individual estimates, which break up the

total into the estimates resulting from their various linear combinations. The method develops here a simple extension of previously used estimators both for one-point estimators as well as two-point estimators or the associated power spectra. Such methods will be useful with future surveys with higher S/N for polarization measurements.

Recently, Calabrese et al. (2009) studied the impact of secondaries in estimation of primordial non-Gaussianity using temperature data. Further studies by Hikage et al. (2010) used Fisher analysis to study joint two-to-one analysis. The estimator introduced above shows how individual linear combination of mixed bispectra can also be used for joint estimation, especially while dealing with non-primordial contamination.

4.2 Power spectra related to the trispectrum

In a recent paper, Munshi et al. (2009) extended the earlier studies by Munshi & Heavens (2010) to the power spectrum related to the trispectrum in an optimal way. This statistic was applied to *WMAP* 5-yr data in Smidt et al. (2010) to provide the first constraints on τ_{NL} and g_{NL} , the third-order corrections to primordial perturbations in non-Gaussian models. The PCLs that we considered before are generalizations of these estimators from the temperature-only case to a fully joint temperature and polarization analysis. For a given choice of a mixed bispectrum, a pair of corresponding power spectra can be defined, which we optimize in this section for arbitrary partial sky coverage and instrumental noise.

4.2.1 Estimator for $K_l^{(3,1)}$

Moving beyond the bispectrum, we can construct estimators of the two power spectra we discussed above, $C_l^{(3,1)}$ and $C_l^{(2,2)}$. We show how to decompose these entire estimators to various choices of mixed bispectra and compress the information optimally to define a unique estimator for each power spectrum. The optimized versions for $K_l^{(3,1)}$ can be constructed by cross-correlating the fields $A^{\mathcal{U}}(r_1, \hat{\Omega})B^{\mathcal{V}}(r_1, \hat{\Omega})B^{\mathcal{W}}(r_2, \hat{\Omega})$ with $B^{\mathcal{X}}(r_2, \hat{\Omega})$. In the first case, the harmonics depend on two radial distances (r_1, r_2) for any given angular direction. For a specific combination of $\mathcal{U}, \mathcal{V}, \mathcal{W}$ and \mathcal{X} , which we can choose either to be temperature T or E-type polarization E , we can define a corresponding estimator. We will eventually combine all various contributions that we recover from these combinations to define a single estimator $K_l^{(3,1)}$, which will generalize the estimator introduced in (Munshi & Heavens 2010) for an analysis of temperature-only data:

$$A^{\mathcal{U}}(r_1)B^{\mathcal{V}}(r_1)|_{lm} = \int A^{\mathcal{U}}(r_1, \hat{\Omega})B^{\mathcal{V}}(r_1, \hat{\Omega})Y_{lm}^*(\hat{\Omega})d\hat{\Omega}; \quad B(r_2)^{\mathcal{X}}|_{lm} = \int B^{\mathcal{X}}(r_2, \hat{\Omega})Y_{lm}^*(\hat{\Omega})d\hat{\Omega}. \quad (61)$$

Next, we construct the field $C^{\mathcal{UV}}(r_1, r_2) = \sum_{lm} F_l(r_1, r_2)A^{\mathcal{U}}(r_1)B^{\mathcal{V}}(r_1)|_{lm}Y_{lm}$. If we now form the product of $C^{\mathcal{UV}}(r_1, r_2)$ and $A^{\mathcal{W}}(r_2)$ and denote it by $D^{\mathcal{UVW}}(r_1, r_2) = C^{\mathcal{UV}}(r_1, r_2)A^{\mathcal{W}}(r_2)$, the spherical harmonic transform of this product field is represented as $D_{lm}^{\mathcal{UVW}}(r_1, r_2)$. Finally, we compute the cross-power spectra between $D^{\mathcal{UVW}}(r_1, r_2)$ and $B^{\mathcal{X}}(r_2)$. We denote it by $\mathcal{J}_l^{A^{\mathcal{U}}B^{\mathcal{V}}A^{\mathcal{W}}B^{\mathcal{X}}}(r_1, r_2)$, which also depends on both radial distances r_1 and r_2 :

$$\mathcal{J}_l^{A^{\mathcal{U}}B^{\mathcal{V}}A^{\mathcal{W}}B^{\mathcal{X}}}(r_1, r_2) = \frac{1}{2l+1} \sum_m \text{Real} \left[\{D^{\mathcal{UVW}}(r_1, r_2)\}_{lm} \{B^{\mathcal{X}}(r_2)\}_{lm}^* \right]. \quad (62)$$

The construction for the second term is very similar. We start by decomposing the real space product $B^{\mathcal{U}}(r, \hat{\Omega})B^{\mathcal{V}}(r, \hat{\Omega})B^{\mathcal{W}}(r, \hat{\Omega})$ and $M^{\mathcal{X}}(r, \hat{\Omega})$ in harmonic space. There is only one radial distance involved in both these terms:

$$B^{\mathcal{U}}(r, \hat{\Omega})B^{\mathcal{V}}(r, \hat{\Omega})B^{\mathcal{W}}(r, \hat{\Omega})|_{lm} = \int [B^{\mathcal{U}}(r, \hat{\Omega})B^{\mathcal{V}}(r, \hat{\Omega})B^{\mathcal{W}}(r, \hat{\Omega})]Y_{lm}^*(\hat{\Omega})d\hat{\Omega}; \quad M^{\mathcal{X}}(r, \hat{\Omega})|_{lm} = \int M^{\mathcal{X}}(r, \hat{\Omega})Y_{lm}^*(\hat{\Omega})d\hat{\Omega}. \quad (63)$$

Finally, the line-of-sight integral, which involves two overlapping contributions through the weighting kernels for the first term and only one for the second, gives us the required estimator:

$$K_l^{(\mathcal{UVW}, \mathcal{X})} = 4f_{\text{nl}}^2 \int r_1^2 dr_1 \int r_2^2 dr_2 \mathcal{J}_l^{A^{\mathcal{U}}B^{\mathcal{V}}A^{\mathcal{W}}B^{\mathcal{X}}}(r_1, r_2) + 2g_{\text{nl}} \int r^2 dr \mathcal{L}_l^{B^{\mathcal{U}}B^{\mathcal{V}}B^{\mathcal{W}}M^{\mathcal{X}}}(r). \quad (64)$$

Next, we show that the construction described above does reduce to an optimum estimator for the power spectrum associated with the trispectrum. The harmonics associated with the product field $B^{\mathcal{U}}(r_1)B^{\mathcal{V}}(r_1)B^{\mathcal{W}}(r_2)$ can be expressed in terms of various $\beta(r)$ functions:

$$B^{\mathcal{U}}(r_1)B^{\mathcal{V}}(r_1)B^{\mathcal{W}}(r_2)|_{lm} = \sum_{LM} (-1)^M \sum_{l_1 m_1, l_2 m_2, l_3 m_3} \tilde{a}_{l_1 m_1}^{\mathcal{U}} \tilde{a}_{l_2 m_2}^{\mathcal{V}} \tilde{a}_{l_3 m_3}^{\mathcal{W}} \alpha_{l_1}^{\mathcal{U}}(r_1) \beta_{l_2}^{\mathcal{V}}(r_1) \alpha_{l_3}^{\mathcal{W}}(r_2) \mathcal{G}_{l_1 l_2 L}^{m_1 m_2 M} \mathcal{G}_{L l_3 l}^{M m_3 m}. \quad (65)$$

The cross-power spectra $\mathcal{J}_l^{ABA, B}(r_1, r_2)$ can be simplified in terms of the following expression:

$$\mathcal{J}_l^{A^{\mathcal{U}}B^{\mathcal{V}}A^{\mathcal{W}}B^{\mathcal{X}}}(r_1, r_2) = \frac{1}{2l+1} \sum_{LM} (-1)^M \sum_m \{F_L(r_1, r_2) \alpha_{l_1}^{\mathcal{U}}(r_1) \beta_{l_2}^{\mathcal{V}}(r_1) \alpha_{l_3}^{\mathcal{W}}(r_2) \beta_l^{\mathcal{X}}(r_2)\} \langle \tilde{a}_{l_1 m_1}^{\mathcal{U}} \tilde{a}_{l_2 m_2}^{\mathcal{V}} \tilde{a}_{l_3 m_3}^{\mathcal{W}} \tilde{a}_{lm}^{\mathcal{X}} \rangle \mathcal{G}_{l_1 l_2 L}^{m_1 m_2 M} \mathcal{G}_{L l_3 l}^{m_3 m M}. \quad (66)$$

The Gaunt integral describing the integral involving three spherical harmonics is defined as follows:

$$\mathcal{G}_{l_1 l_2 l_3}^{m_1 m_2 m_3} = \sqrt{\frac{(2l_1+1)(2l_2+1)(2l_3+1)}{4\pi}} \begin{pmatrix} l_1 & l_2 & l_3 \\ 0 & 0 & 0 \end{pmatrix} \begin{pmatrix} l_1 & l_2 & l_3 \\ m_1 & m_2 & m_3 \end{pmatrix}. \quad (67)$$

The second terms can be treated in an analogous way and the result takes the following form:

$$\mathcal{L}_l^{B^{\mathcal{U}}B^{\mathcal{V}}M^{\mathcal{W}}B^{\mathcal{X}}}(r) = \frac{1}{2l+1} \sum_{LM} (-1)^M \sum_m \{\beta_{l_1}^{\mathcal{U}}(r) \beta_{l_2}^{\mathcal{V}}(r) \mu_{l_3}^{\mathcal{W}}(r) \beta_l^{\mathcal{X}}(r)\} \langle \tilde{a}_{l_1 m_1}^{\mathcal{U}} \tilde{a}_{l_2 m_2}^{\mathcal{V}} \tilde{a}_{l_3 m_3}^{\mathcal{W}} \tilde{a}_{lm}^{\mathcal{X}} \rangle \mathcal{G}_{l_1 l_2 L}^{m_1 m_2 M} \mathcal{G}_{L l_3 l}^{m_3 m M}. \quad (68)$$

Finally, when these terms are combined, as in equation (64), we recover the following expression:

$$\hat{\mathcal{K}}_l^{(\mathcal{UVW}, \mathcal{X})} = \frac{1}{2l+1} \sum_{l_1 l_2 l_3} \sum_L \frac{1}{(2L+1)} [\mathbf{C}^{-1}]_{l_1}^{\mathcal{U}\mathcal{U}'} [\mathbf{C}^{-1}]_{l_2}^{\mathcal{V}\mathcal{V}'} [\mathbf{C}^{-1}]_{l_3}^{\mathcal{W}\mathcal{W}'} [\mathbf{C}^{-1}]_l^{\mathcal{X}\mathcal{X}'} T_{\mathcal{W}_3 \mathcal{X}_4'}^{\mathcal{U}_1 \mathcal{V}_2} [L] \left[\hat{T}_{\mathcal{W}_3 \mathcal{X}_4'}^{\mathcal{U}_1 \mathcal{V}_2} [L] - \hat{G}_{\mathcal{W}_3 \mathcal{X}_4'}^{\mathcal{U}_1 \mathcal{V}_2} [L] \right]. \quad (69)$$

We have subtracted the Gaussian component from the estimator in the last step. This is done by simulating Gaussian maps in a MC chain and using the same mask and the noise as the real data, weighting functions used for real data are also used on the Gaussian realizations. The ensemble averages of the Gaussian realizations are then subtracted from the estimates from the real data.

We can sum over all possible mixed bispectra to construct the following combined estimator:

$$\hat{\mathcal{K}}_l^{(3,1)} = \sum_{\mathcal{UVW}\mathcal{X}} \hat{\mathcal{K}}_l^{(\mathcal{UVW}, \mathcal{X})}. \quad (70)$$

The estimator $\hat{\mathcal{K}}_l^{(\mathcal{UVW}, \mathcal{X})}$ depends linearly both on f_{NL}^2 and g_{NL} . In principle, we can use the estimate of f_{NL} from a bispectrum analysis as a prior, or we can use the estimators $\mathcal{S}_l^{(2,1)}$, $\mathcal{K}_l^{(3,1)}$ and $\mathcal{K}_l^{(3,1)}$ to put joint constraints on f_{NL} and g_{NL} . The former is better from an S/N point of view (Smidt et al. 2010). Computational evaluation of either of the power spectra clearly will be more involved as a double integral corresponding to two radial directions needs to be evaluated. Given the low S/N associated with these power spectra, binning will be essential.

4.2.2 Estimator for $\mathcal{K}_l^{(\mathcal{UV}, \mathcal{WX})}$

In an analogous way, the other power spectra associated with the trispectrum can be optimized by the following construction. We start by taking the harmonic transform of the product field $A(r, \hat{\Omega})B(r, \hat{\Omega})$ evaluated at the same line-of-sight distance r :

$$A^{\mathcal{U}}(r, \hat{\Omega})B^{\mathcal{V}}(r, \hat{\Omega})|_{lm} = \int A^{\mathcal{U}}(r)B^{\mathcal{V}}(r)Y_{lm}^*(\hat{\Omega})d\hat{\Omega}; \quad B^{\mathcal{W}}(r, \hat{\Omega})M^{\mathcal{X}}(r, \hat{\Omega})|_{lm} = \int B^{\mathcal{W}}(r)M^{\mathcal{X}}(r)Y_{lm}^*(\hat{\Omega})d\hat{\Omega}, \quad (71)$$

and contract it with its counterpart at a different distance. The corresponding power spectrum (which is a function of these two line-of-sight distances r_1 and r_2) has the first term

$$\mathcal{J}_l^{A^{\mathcal{U}}B^{\mathcal{V}}, A^{\mathcal{W}}B^{\mathcal{X}}}(r_1, r_2) = \frac{1}{2l+1} \sum_m F_l(r_1, r_2) A^{\mathcal{U}}(r_1, \hat{\Omega}) B^{\mathcal{V}}(r_1, \hat{\Omega})|_{lm} A(r_2, \hat{\Omega})^{\mathcal{W}} B(r_2, \hat{\Omega})^{\mathcal{X}}|_{lm}^*. \quad (72)$$

Similarly, the second part of the contribution can be constructed by cross-correlating the product of three-dimensional fields $B^{\mathcal{U}}(\hat{\Omega}, r_1)B^{\mathcal{V}}(\hat{\Omega}, r_1)$ against $B^{\mathcal{W}}(\hat{\Omega}, r_2)M^{\mathcal{X}}(\hat{\Omega}, r_2)$ evaluated at the same radial distance r :

$$\mathcal{L}_l^{B^{\mathcal{U}}B^{\mathcal{V}}, B^{\mathcal{W}}M^{\mathcal{X}}}(r) = \frac{1}{2l+1} \sum_m B^{\mathcal{U}}(r, \hat{\Omega})B^{\mathcal{V}}(r, \hat{\Omega})|_{lm} B^{\mathcal{W}}(r, \hat{\Omega})M^{\mathcal{X}}(r, \hat{\Omega})|_{lm}^*. \quad (73)$$

Finally, the estimator is constructed by integrating along the line-of-sight distances:

$$\hat{\mathcal{K}}_l^{(\mathcal{UV}, \mathcal{WX})} = 4f_{\text{nl}}^2 \int r_1^2 dr_1 \int r_2^2 dr_2 \mathcal{J}_l^{A^{\mathcal{U}}B^{\mathcal{V}}, A^{\mathcal{W}}B^{\mathcal{X}}}(r_1, r_2) + 2g_{\text{nl}} \int r^2 dr \mathcal{L}_l^{B^{\mathcal{U}}B^{\mathcal{V}}, B^{\mathcal{W}}M^{\mathcal{X}}}(r). \quad (74)$$

To see they do correspond to an optimum estimator, we use the harmonic expansions and follow the same procedure as outlined before:

$$\mathcal{L}_l^{B^{\mathcal{U}}B^{\mathcal{V}}, B^{\mathcal{W}}M^{\mathcal{X}}}(r) = \frac{1}{2l+1} \sum_m (-1)^m \sum_{l_1 m_1} \{ \beta_{l_1}^{\mathcal{U}}(r) \beta_{l_2}^{\mathcal{V}}(r) \beta_{l_3}^{\mathcal{W}}(r) \mu_{l_4}^{\mathcal{X}}(r) \} \langle \tilde{a}_{l_1 m_1}^{\mathcal{U}} \tilde{a}_{l_2 m_2}^{\mathcal{V}} \tilde{a}_{l_3 m_3}^{\mathcal{W}} \tilde{a}_{l_4 m_4}^{\mathcal{X}} \rangle \mathcal{G}_{l_1 l_2 l}^{m_1 m_2 m} \mathcal{G}_{l_3 l_4 l}^{m_3 m_4 m}. \quad (75)$$

$$\mathcal{J}_l^{A^{\mathcal{U}}B^{\mathcal{V}}, A^{\mathcal{W}}B^{\mathcal{X}}}(r_1, r_2) = \frac{1}{2l+1} \sum_m (-1)^m \sum_{l_1 m_1} \{ F_l(r_1, r_2) \alpha_{l_1}^{\mathcal{U}}(r_1) \beta_{l_2}^{\mathcal{V}}(r_1) \alpha_{l_3}^{\mathcal{W}}(r_2) \beta_{l_4}^{\mathcal{X}}(r_2) \} \langle \tilde{a}_{l_1 m_1}^{\mathcal{U}} \tilde{a}_{l_2 m_2}^{\mathcal{V}} \tilde{a}_{l_3 m_3}^{\mathcal{W}} \tilde{a}_{l_4 m_4}^{\mathcal{X}} \rangle \mathcal{G}_{l_1 l_2 l}^{m_1 m_2 m} \mathcal{G}_{l_3 l_4 l}^{m_3 m_4 m}. \quad (76)$$

Here, we notice that $\mathcal{J}_l^{AB, AB}(r_1, r_2)$ is invariant under exchange of r_1 and r_2 , but $\mathcal{J}_l^{BB, BM}(r_1, r_2)$ is not. Finally, joining the various contributions to construct the final estimator, as given in equation (74), which involves a line-of-sight integration:

$$\hat{\mathcal{K}}_l^{(\mathcal{UV}, \mathcal{WX})} = \frac{1}{2l+1} \sum_{\mathcal{U}'\mathcal{V}'\mathcal{W}'\mathcal{X}'} \sum_{l_1 m_1} \frac{1}{(2l+1)} [\mathbf{C}^{-1}]_{l_1}^{\mathcal{U}\mathcal{U}'} [\mathbf{C}^{-1}]_{l_2}^{\mathcal{V}\mathcal{V}'} [\mathbf{C}^{-1}]_{l_3}^{\mathcal{W}\mathcal{W}'} [\mathbf{C}^{-1}]_l^{\mathcal{X}\mathcal{X}'} T_{\mathcal{W}_3 \mathcal{X}_4'}^{\mathcal{U}_1 \mathcal{V}_2} (l) \left[\hat{T}_{\mathcal{W}_3 \mathcal{X}_4'}^{\mathcal{U}_1 \mathcal{V}_2} (l) - \hat{G}_{\mathcal{W}_3 \mathcal{X}_4'}^{\mathcal{U}_1 \mathcal{V}_2} (l) \right], \quad (77)$$

and the combined estimator

$$\mathcal{K}_l^{(2,2)} = \sum_{\mathcal{UVW}\mathcal{X}} \mathcal{K}_l^{(\mathcal{UV}, \mathcal{WX})}. \quad (78)$$

The pre-factors associated with f_{NL}^2 and g_{NL} are different in the linear combinations $\mathcal{K}_l^{(2,2)}$ and $\mathcal{K}_l^{(3,1)}$, and hence even without using information from the third order, we can estimate both from the fourth order alone. Fig. 4 shows a plot of $\mathcal{K}_l^{(3,1)}$ and $\mathcal{K}_l^{(2,2)}$.

Similarly, the one-point cumulant involving both temperature and E-type polarization at the fourth order can be written in terms of the mixed trispectra as follows:

$$\hat{\mathcal{K}}_l^{(4)} = \sum_l (2l+1) \hat{\mathcal{K}}_l^{(2,2)} = \sum_l (2l+1) \sum_{\mathcal{UVW}\mathcal{X}} \hat{\mathcal{K}}_l^{(\mathcal{UV}, \mathcal{WX})} = \sum_l (2l+1) \hat{\mathcal{K}}_l^{(3,1)} = \sum_l (2l+1) \sum_{\mathcal{UVW}\mathcal{X}} \hat{\mathcal{K}}_l^{(\mathcal{UVW}, \mathcal{X})}. \quad (79)$$

It is also possible to carry out the sum over the harmonics l without summing over the field types. In this case, we recover independent one-point estimators associated with each type of mixed trispectra:

$$\hat{\mathcal{K}}^{\mathcal{UVW}\mathcal{X}} = \sum_l (2l+1) \hat{\mathcal{K}}_l^{(\mathcal{UV}, \mathcal{WX})} = \sum_l (2l+1) \hat{\mathcal{K}}_l^{(\mathcal{UVW}, \mathcal{X})}. \quad (80)$$

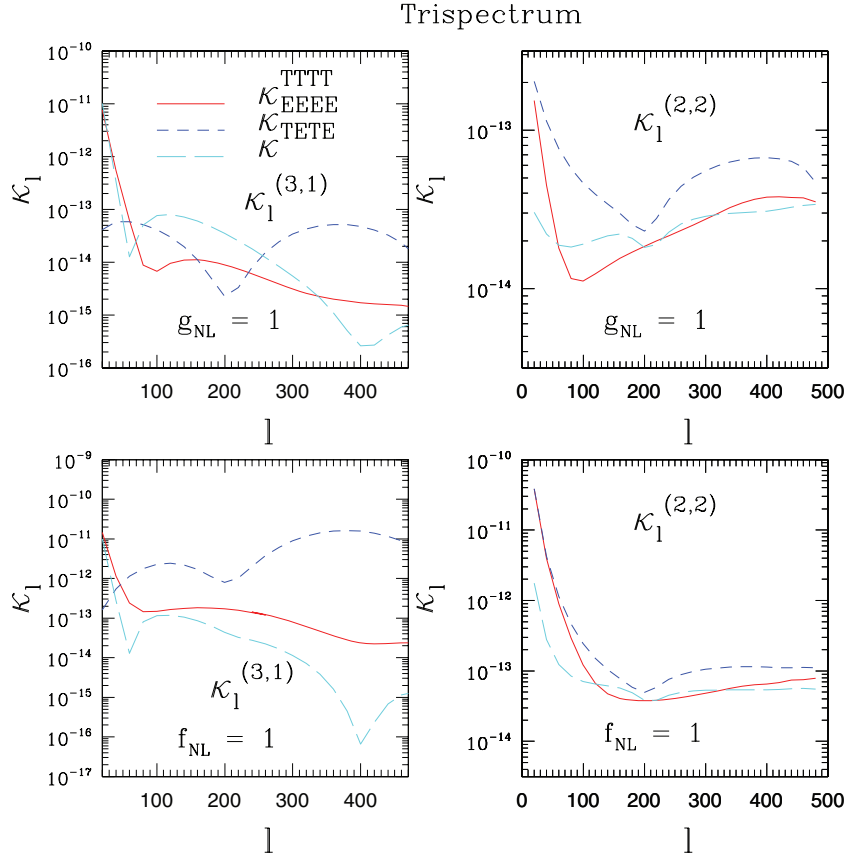


Figure 4. Various trispectrum-related power spectra are plotted as a function of the angular scale. An ideal all-sky no-noise experimental set-up was used for computing the power spectra. Three different trispectra were considered for the combinations $TTTT$, $EEEE$ and $TETE$. The left-hand panels correspond to the estimator $(2l+1)\kappa_l^{(3,1)}$ and the right-hand panels correspond to $(2l+1)\kappa_l^{(2,2)}$. Upper panels correspond to $g_{\text{NL}} = 1$ and the bottom panels correspond to $f_{\text{NL}} = 1$. Cosmological parameters correspond to that of *WMAP7* analysis (Larson et al. 2010). See text for details.

We will next consider the correction terms for these estimators due to absence of spherical symmetry – which may be broken either because of mask or because of the presence of detector noise in an arbitrary scanning strategy.

4.3 Correction in the absence of spherical symmetry

It was pointed out in Babich (2005), Creminelli et al. (2006) and Yadav et al. (2008) that in the presence of a partial sky coverage, for example, due to the presence of a mask or because of the galactic foregrounds and the bright point sources, as well as, in the case of non-uniform noise, spherical symmetry is destroyed. The estimators introduced above will then have to be modified by adding terms, which are linear in the observed map. The corrective terms are incorporated using MC techniques. A more general treatment, which involves computationally expensive inverse-covariance weighting, will be discussed later. The treatment discussed here is nearly optimal though ignores mode–mode coupling dominant at low ℓ .

4.3.1 Corrective terms for $C_l^{\mathcal{U}, \mathcal{V}\mathcal{W}}$

The (linear) corrective terms are constructed from correlating the MC-averaged $\langle A^{\mathcal{U}}(r, \hat{\Omega})B^{\mathcal{V}}(r, \hat{\Omega}) \rangle_{\text{sim}}$ product maps with the input $B^{\mathcal{W}}(r, \hat{\Omega})$ map. The mask and the noise that are used in constructing the MC-averaged product map are exactly the same as the observed maps and the ones derived from them, such as A or B .

Mode–mode coupling is important at low angular modes, and we consider the full case later, but for higher frequency modes, we can approximate the linear correction to the local shape:

$$\begin{aligned} \hat{C}_l^{A^{\mathcal{U}}B^{\mathcal{V}}B^{\mathcal{W}}} &= \frac{1}{f_{\text{sky}}} \left\{ \hat{C}_l^{A^{\mathcal{U}}, B^{\mathcal{V}}B^{\mathcal{W}}} - C_l^{(A^{\mathcal{U}}, B^{\mathcal{V}})B^{\mathcal{W}}} - C_l^{(A^{\mathcal{U}}, B^{\mathcal{W}})B^{\mathcal{V}}} - C_l^{A^{\mathcal{U}}, (B^{\mathcal{V}}B^{\mathcal{W}})} \right\} \\ &+ \frac{1}{f_{\text{sky}}} \left\{ \hat{C}_l^{A^{\mathcal{U}}B^{\mathcal{V}}, B^{\mathcal{W}}} - C_l^{(A^{\mathcal{U}}B^{\mathcal{V}}), B^{\mathcal{W}}} - C_l^{B^{\mathcal{V}}(A^{\mathcal{U}}, B^{\mathcal{W}})} - C_l^{A^{\mathcal{U}}(B^{\mathcal{V}}, B^{\mathcal{W}})} \right\} \\ &+ \frac{1}{f_{\text{sky}}} \left\{ \hat{C}_l^{A^{\mathcal{U}}B^{\mathcal{W}}, B^{\mathcal{V}}} - C_l^{(A^{\mathcal{U}}B^{\mathcal{W}}), B^{\mathcal{V}}} - C_l^{B^{\mathcal{W}}(A^{\mathcal{U}}, B^{\mathcal{V}})} - C_l^{A^{\mathcal{U}}(B^{\mathcal{W}}, B^{\mathcal{V}})} \right\}, \end{aligned} \quad (81)$$

where f_{sky} is the observed sky fraction.

The C_l , such as $C_l^{(AB),B}$, describe the cross-power spectra associated with MC-averaged product maps $\langle A(n, r)B(n, r) \rangle$ constructed with the same mask and the noise model as the observed map B . Likewise, the term $C_l^{A(B,B)}$ denotes the average cross-correlation computed from MC averaging of the product map constructed from the observed map $A(\Omega, r)$ multiplied with an MC realization of map $B(\Omega, r)$ against the same MC realization $B(\Omega, r)$. Creminelli et al. (2006) showed via numerical analysis that the linear terms are less important in the equilateral case than in the local model. The use of such MC maps to model the effect of mask and noise greatly improves the speed compared to full bispectrum analysis.

The use of linear terms was found to greatly reduce the scatter of this estimator, thereby improving its optimality. The estimator was used in Yadav & Wandelt (2008) also to compute f_{NL} from combined T and E maps. The analysis presented above is approximate, because it uses a crude f_{sky} approximation to deconvolve the estimated power spectrum to compare with analytical prediction. A more accurate analysis should take into account the mode–mode coupling, which can dominate at low l . The speed of this analysis depends on how fast we can generate non-Gaussian maps. The general expression, which includes the mode–mode coupling, will be presented in the next section. However, it was found by Yadav & Wandelt (2008) that removing low modes of l from the analysis can be an efficient way to bypass the mode–mode coupling. A complete numerical treatment for the case of two-point statistics, such as C_l^{A,B^2} , will be presented elsewhere.

4.3.2 Corrective terms for the estimator $\mathcal{K}_l^{\mathcal{UVW},\mathcal{X}}$

For the four-point terms, we need to subtract linear and quadratic terms:

$$\hat{\mathcal{J}}_l^{A_1^{\mathcal{U}} B_1^{\mathcal{V}} A_2^{\mathcal{W}} B_2^{\mathcal{X}}} = \frac{1}{f_{\text{sky}}} \left[\tilde{\mathcal{J}}_l^{A_1^{\mathcal{U}} B_1^{\mathcal{V}} A_2^{\mathcal{W}} B_2^{\mathcal{X}}} - \mathcal{I}_l^{\text{Lin}} - \mathcal{I}_l^{\text{Quad}} \right] \quad (82)$$

$$\mathcal{I}_l^{\text{Lin}} = \frac{1}{f_{\text{sky}}} \left[\mathcal{J}_l^{(A_1^{\mathcal{U}} B_1^{\mathcal{V}} A_2^{\mathcal{W}}), B_2^{\mathcal{X}}} + \mathcal{J}_l^{(A_1^{\mathcal{U}} B_1^{\mathcal{V}} A_2^{\mathcal{W}}), B_2^{\mathcal{X}}} + \mathcal{J}_l^{(B_1^{\mathcal{V}} A_1^{\mathcal{U}} A_2^{\mathcal{W}}), B_2^{\mathcal{X}}} + \mathcal{J}_l^{(A_2^{\mathcal{W}} A_1^{\mathcal{U}} B_1^{\mathcal{V}}), B_2^{\mathcal{X}}} \right] \quad (83)$$

$$\mathcal{I}_l^{\text{Quad}} = \frac{1}{f_{\text{sky}}} \left[\mathcal{J}_l^{(A_1^{\mathcal{U}} B_1^{\mathcal{V}} A_2^{\mathcal{W}}), B_2^{\mathcal{X}}} + \mathcal{J}_l^{(A_1^{\mathcal{U}} A_2^{\mathcal{W}}), B_1^{\mathcal{V}} B_2^{\mathcal{X}}} + \mathcal{J}_l^{(B_1^{\mathcal{V}} A_2^{\mathcal{W}}), A_1^{\mathcal{U}} B_2^{\mathcal{X}}} + \mathcal{J}_l^{(A_1^{\mathcal{U}} B_1^{\mathcal{V}}), A_2^{\mathcal{W}} B_2^{\mathcal{X}}} + \mathcal{J}_l^{(A_2^{\mathcal{W}} B_1^{\mathcal{V}}), A_1^{\mathcal{U}} B_2^{\mathcal{X}}} + \mathcal{J}_l^{(B_1^{\mathcal{V}} A_2^{\mathcal{W}}), A_1^{\mathcal{U}} B_2^{\mathcal{X}}} \right]. \quad (84)$$

The expressions are similar for the other terms that depend on only one radial distance:

$$\hat{\mathcal{L}}_l^{B^{\mathcal{U}} B^{\mathcal{V}} M^{\mathcal{W}}, B^{\mathcal{X}}} = \frac{1}{f_{\text{sky}}} \left[\tilde{\mathcal{L}}_l^{B^{\mathcal{U}} B^{\mathcal{V}} M^{\mathcal{W}}, B^{\mathcal{X}}} - \mathcal{I}_l^{\text{Lin}} - \mathcal{I}_l^{\text{Quad}} \right] \quad (85)$$

$$\mathcal{I}_l^{\text{Lin}} = \frac{1}{f_{\text{sky}}} \left[\mathcal{L}_l^{(B^{\mathcal{U}} B^{\mathcal{V}} M^{\mathcal{W}}), B^{\mathcal{X}}} + \mathcal{L}_l^{(B^{\mathcal{U}} B^{\mathcal{V}} M^{\mathcal{W}}), B^{\mathcal{X}}} + \mathcal{L}_l^{(B^{\mathcal{U}} B^{\mathcal{V}} M^{\mathcal{W}}), B^{\mathcal{X}}} + \mathcal{L}_l^{(B^{\mathcal{U}} B^{\mathcal{V}} M^{\mathcal{W}}), B^{\mathcal{X}}} \right] \quad (86)$$

$$\mathcal{I}_l^{\text{Quad}} = \frac{1}{f_{\text{sky}}} \left[\mathcal{L}_l^{(B^{\mathcal{U}} B^{\mathcal{V}} M^{\mathcal{W}}), B^{\mathcal{X}}} + \mathcal{L}_l^{(B^{\mathcal{U}} B^{\mathcal{V}} M^{\mathcal{W}}), B^{\mathcal{X}}} + \mathcal{L}_l^{(B^{\mathcal{U}} B^{\mathcal{V}} M^{\mathcal{W}}), B^{\mathcal{X}}} + \mathcal{L}_l^{(B^{\mathcal{U}} B^{\mathcal{V}} M^{\mathcal{W}}), B^{\mathcal{X}}} + \mathcal{L}_l^{(B^{\mathcal{U}} B^{\mathcal{V}} M^{\mathcal{W}}), B^{\mathcal{X}}} + \mathcal{L}_l^{(B^{\mathcal{U}} B^{\mathcal{V}} M^{\mathcal{W}}), B^{\mathcal{X}}} \right]. \quad (87)$$

To simplify the presentation, we have used the symbol $A^{\mathcal{U}}(r_1, \hat{\Omega}) = A_1^{\mathcal{U}}; A^{\mathcal{U}}(r, \hat{\Omega}) = A^{\mathcal{U}}$ and so on. Essentially, we can see that there are terms, which are linear in the input harmonics, and terms, which are quadratic in the input harmonics. The terms, which are linear, are also proportional to the bispectrum of the remaining three-dimensional fields, which are being averaged. On the other hand, the prefactors for quadratic terms are three-dimensional correlation functions of the remaining two fields. Finally, putting all of these expressions, we can write

$$\tilde{\mathcal{K}}_l^{\mathcal{UVW},\mathcal{X}} = 4f_{\text{NL}}^2 \int r_1^2 dr_1 \int r_2^2 dr_2 \tilde{\mathcal{J}}_l^{A_1^{\mathcal{U}} B_1^{\mathcal{V}} A_2^{\mathcal{W}} B_2^{\mathcal{X}}}(r_1, r_2) + 2g_{\text{NL}} \int r^2 dr \tilde{\mathcal{L}}_l^{B^{\mathcal{U}} B^{\mathcal{V}} M^{\mathcal{W}}, B^{\mathcal{X}}}(r). \quad (88)$$

From a computational point of view, clearly, the overlap integral $F_L(r_1, r_2)$ will be expensive and may determine to what resolution ultimately these direct techniques can be implemented. Use of these techniques directly involving MC numerical simulations will be dealt with in a separate paper (Smidt et al., in preparation). To what extent the linear and quadratic terms are important in each of these contributions can only be decided by testing against simulation.

4.3.3 Corrective terms for the estimator $\mathcal{K}_l^{\mathcal{UV},\mathcal{W},\mathcal{X}}$

The unbiased estimator for the other estimator can be constructed in a similar manner. As before, there are terms which are quadratic in input harmonics with a prefactor proportional to terms involving cross-correlation or variance of various combinations of three-dimensional fields and there will be linear terms (linear in input harmonics) with a pre-factor proportional to the bispectrum associated with various three-dimensional fields:

$$\hat{\mathcal{J}}_l^{A_1^{\mathcal{U}} B_1^{\mathcal{V}} A_2^{\mathcal{W}} B_2^{\mathcal{X}}} = \frac{1}{f_{\text{sky}}} \left[\tilde{\mathcal{J}}_l^{A_1^{\mathcal{U}} B_1^{\mathcal{V}} A_2^{\mathcal{W}} B_2^{\mathcal{X}}} - \mathcal{I}_l^{\text{Lin}} - \mathcal{I}_l^{\text{Quad}} \right] \quad (89)$$

$$\mathcal{I}_l^{\text{Lin}} = \frac{1}{f_{\text{sky}}} \left[\mathcal{J}_l^{(A_1^{\mathcal{U}} B_1^{\mathcal{V}}), (A_2^{\mathcal{W}} B_2^{\mathcal{X}})} + \mathcal{J}_l^{(A_1^{\mathcal{U}} B_1^{\mathcal{V}}), A_2^{\mathcal{W}} B_2^{\mathcal{X}}} + \mathcal{J}_l^{(A_1^{\mathcal{U}} B_1^{\mathcal{V}}), B_2^{\mathcal{X}} A_2^{\mathcal{W}}} + \mathcal{J}_l^{(B_1^{\mathcal{V}} A_1^{\mathcal{U}}), A_2^{\mathcal{W}} B_2^{\mathcal{X}}} + \mathcal{J}_l^{(B_1^{\mathcal{V}} A_1^{\mathcal{U}}), B_2^{\mathcal{X}} A_2^{\mathcal{W}}} + \mathcal{J}_l^{(B_1^{\mathcal{V}} A_1^{\mathcal{U}}), B_2^{\mathcal{X}}} \right] \quad (90)$$

$$\mathcal{I}^{\text{Quad}} = \frac{1}{f_{\text{sky}}} \left[\mathcal{J}_l^{A_1^{\mathcal{U}}(B_1^{\mathcal{V}}, A_2^{\mathcal{V}} B_2^{\mathcal{X}})} + \mathcal{J}_l^{B_1^{\mathcal{V}}(A_1^{\mathcal{U}}, A_2^{\mathcal{V}} B_2^{\mathcal{X}})} + \mathcal{J}_l^{A_1^{\mathcal{U}} B_1^{\mathcal{V}}, A_2^{\mathcal{V}} B_2^{\mathcal{X}}} + \mathcal{J}_l^{A_1^{\mathcal{U}} B_1^{\mathcal{V}}, B_2^{\mathcal{X}} A_2^{\mathcal{V}}} \right]. \quad (91)$$

The terms, such as $\mathcal{K}_l^{AB, BM}(r_1, r_2)$, can be constructed in a very similar way. We display the term $\mathcal{K}_l^{AB^2, A}(r_1, r_2)$ with all its corrections included:

$$\hat{\mathcal{L}}_l^{B^{\mathcal{U}} B^{\mathcal{V}}, B^{\mathcal{W}} M^{\mathcal{X}}} = \frac{1}{f_{\text{sky}}} \left[\tilde{\mathcal{L}}_l^{B^{\mathcal{U}} B^{\mathcal{V}}, B^{\mathcal{W}} M^{\mathcal{X}}} - I_l^{\text{Lin}} - I_l^{\text{Quad}} \right] \quad (92)$$

$$I_l^{\text{Quad}} = \frac{1}{f_{\text{sky}}} \left[\mathcal{L}_l^{B^{\mathcal{U}}(B^{\mathcal{V}} B^{\mathcal{W}}), M^{\mathcal{X}}} + \mathcal{L}_l^{B^{\mathcal{V}}(B^{\mathcal{U}}, B^{\mathcal{W}}) M^{\mathcal{X}}} + \mathcal{L}_l^{B^{\mathcal{W}}(B^{\mathcal{V}}, B^{\mathcal{U}}) M^{\mathcal{X}}} + \mathcal{K}_l^{B^{\mathcal{U}} B^{\mathcal{V}}(B^{\mathcal{W}}, M^{\mathcal{X}})} + \mathcal{K}_l^{B^{\mathcal{W}} B^{\mathcal{V}}(B^{\mathcal{U}}, M^{\mathcal{X}})} + \mathcal{K}_l^{B^{\mathcal{U}} B^{\mathcal{W}}(B^{\mathcal{V}}, M^{\mathcal{X}})} \right] \quad (93)$$

$$I_l^{\text{Lin}} = \frac{1}{f_{\text{sky}}} \left[\mathcal{J}_l^{B^{\mathcal{U}}(B^{\mathcal{V}}, B^{\mathcal{W}} M^{\mathcal{X}})} + \mathcal{J}_l^{B^{\mathcal{V}}(B^{\mathcal{U}}, B^{\mathcal{W}} M^{\mathcal{X}})} + \mathcal{J}_l^{B^{\mathcal{W}}(B^{\mathcal{V}}, B^{\mathcal{U}} M^{\mathcal{X}})} + \mathcal{J}_l^{B^{\mathcal{U}} B^{\mathcal{V}}, B^{\mathcal{W}} M^{\mathcal{X}}} \right]. \quad (94)$$

The importance of the linear terms depends greatly on the target model being considered. For example, while linear terms for bispectral analysis can greatly reduce the amount of scatter in the estimator for *local* non-Gaussianity, the linear term is less important in modelling the *equilateral* model. In any case, the use of such MC maps is known to reduce the scatter and can greatly simplify the estimation of non-Gaussianity. This can be useful, as fully optimal analysis with inverse-variance weighting, which treats mode–mode coupling completely, may only be possible on low-resolution maps:

$$\tilde{\mathcal{K}}_l^{(\mathcal{U}\mathcal{V}, \mathcal{W}\mathcal{X})} = 4f_{\text{NL}}^2 \int r_1^2 dr_1 \int r_2 dr_2 \tilde{\mathcal{J}}_l^{A^{\mathcal{U}} B^{\mathcal{V}}, A^{\mathcal{W}} B^{\mathcal{X}}}(r_1, r_2) + 2g_{\text{NL}} \int r^2 dr \tilde{\mathcal{L}}_l^{B^{\mathcal{U}} B^{\mathcal{V}}, B^{\mathcal{W}} M^{\mathcal{X}}}(r). \quad (95)$$

The corrections to one-point estimators can be recovered by performing appropriate sums. In the next section, we use direct summations and proper modelling of the covariance matrix as opposed to the MC techniques used here. However, in certain situations, it may be difficult to model the covariance matrix in an accurate way. We also provide analytical results, which can handle such situations.

5 EXACT ANALYSIS OF OPTIMAL ESTIMATORS

In the previous section, we relied on MC simulations to model the effect of finite sky coverage, noise as well as other observational artefacts. The resulting method is nearly optimal and for most cases, where mode–mode coupling is not too strong, that is, for near all-sky coverage, it can be efficient. To take mode–mode coupling properly into account, which is the case for low multipoles, we need to model the covariance matrix as accurately as we can. In this section, we tackle the case, where inverse-covariance weighting is required. The resulting method is optimal and can provide accurate results for studies with degraded resolution maps, where cross-contamination to primordial non-Gaussianities coming from secondaries is minimum.

5.1 The power spectrum related to the bispectrum

The general expression for the bispectrum estimator was developed by Babich (2005) for arbitrary sky coverage and inhomogeneous noise. The estimator includes a cubic term, which by matched-filtering maximizes the response for a specific type of input map bispectrum. The speed of this analysis depends on how fast we can generate non-Gaussian maps. The linear terms vanish in the absence of anisotropy, but should be included for realistic noise to reduce the scatter in the estimates (see Babich 2005 for details). We define the optimal estimator as

$$\begin{aligned} \hat{E}_L^{\mathcal{X}, \mathcal{Y}, \mathcal{Z}}[a] = \sum_{L'} [N^{-1}]_{LL'} & \left[\frac{1}{6} \sum_{\mathcal{X}' \mathcal{Y}' \mathcal{Z}'} \sum_{M M'} \sum_{l' l_1 m m_1} B_{L' l' l'}^{\mathcal{X} \mathcal{Y} \mathcal{Z}} \begin{pmatrix} L' & l & l' \\ M' & m & m' \end{pmatrix} \right. \\ & \times \left\{ \left([C_{L' M', l_1 m_1}^{-1}]^{\mathcal{X} \mathcal{X}} a_{l_1 m_1}^{\mathcal{X}'} \right) \left([C_{l m, l_2 m_2}^{-1}]^{\mathcal{Y} \mathcal{Y}'} a_{l_2 m_2}^{\mathcal{Y}'} \right) \left([C_{l' m', l_3 m_3}^{-1}]^{\mathcal{Z} \mathcal{Z}'} a_{l_3 m_3}^{\mathcal{Z}'} \right) \right. \\ & \left. \left. - [C_{l m, l' m'}^{-1}]^{\mathcal{X} \mathcal{Y}} \left([C_{L' M', l_2 m_2}^{-1}]^{\mathcal{Z} \mathcal{Z}'} a_{l_2 m_2}^{\mathcal{Z}'} \right) - [C_{L M, l m}^{-1}]^{\mathcal{X} \mathcal{Z}} \left([C_{l' m', l_2 m_2}^{-1}]^{\mathcal{Y} \mathcal{Y}'} a_{l_2 m_2}^{\mathcal{Y}'} \right) - [C_{L M, l m}^{-1}]^{\mathcal{Y} \mathcal{Z}} \left([C_{l' m', l_2 m_2}^{-1}]^{\mathcal{X} \mathcal{X}'} a_{l_2 m_2}^{\mathcal{X}'} \right) \right\} \right]; \\ & \mathcal{X}, \mathcal{Y}, \mathcal{Z}, \mathcal{X}', \mathcal{Y}', \mathcal{Z}' \in \{T, E\}, \end{aligned} \quad (96)$$

where $N_{LL'}$ is a normalization to be discussed later. A factor of $1/(2l+1)$ can be introduced with the sum \sum_M , if we choose not to introduce the $N_{LL'}$ normalization constant. This will make the estimator equivalent to the one introduced in the previous section. As the data are weighted by $C^{-1} = (S + N)^{-1}$, or the inverse-covariance matrix, the speed of this analysis depends on how quickly we can generate non-Gaussian maps. Addition of higher modes will reduce the variance of the estimator. In contrast, the performance of suboptimal estimators can degrade with resolution, due to the presence of inhomogeneous noise or a galactic mask. However, an incorrect noise covariance matrix can not only make the estimator suboptimal, but it will also make the estimator biased. The noise model will depend on the specific survey scan strategy. Numerical implementation of such inverse-variance weighting or multiplication of a map by C^{-1} can be carried out by conjugate gradient inversion techniques. Taking clues from Smith & Zaldarriaga (2006), we extend their estimators for the case of the skew spectrum. We will be closely following their notation whenever possible. First, we define $Q_L[a]$ and its derivative $\partial_{lm} Q_L[a]$. The required input harmonics a_{lm}

are denoted as a :

$$\hat{Q}_L^{\mathcal{X},\mathcal{Y}\mathcal{Z}}[a] \equiv \frac{1}{6} \sum_M a_{LM}^{\mathcal{X}} \sum_{l'm',l''m''} B_{Ll'l''}^{\mathcal{X}\mathcal{Y}\mathcal{Z}} \begin{pmatrix} L & l' & l'' \\ M & m' & m'' \end{pmatrix} a_{l'm'}^{\mathcal{Y}} a_{l''m''}^{\mathcal{Z}}; \quad (97)$$

$$\partial_{lm}^{\mathcal{X}} \hat{Q}_L^{\mathcal{X},\mathcal{Y}\mathcal{Z}}[a] \equiv \frac{1}{6} \delta_{Ll} \sum_{l'm',l''m''} B_{Ll'l''}^{\mathcal{X}\mathcal{Y}\mathcal{Z}} \begin{pmatrix} L & l' & l'' \\ m & m' & m'' \end{pmatrix} a_{l'm'}^{\mathcal{Y}} a_{l''m''}^{\mathcal{Z}}; \quad (98)$$

$$\partial_{lm}^{\mathcal{Y}/\mathcal{Z}} \hat{Q}_L^{\mathcal{X},\mathcal{Y}\mathcal{Z}}[a] \equiv \frac{1}{6} \sum_M a_{LM}^{\mathcal{X}} \sum_{l'm'} B_{Ll'l'}^{\mathcal{X}\mathcal{Y}\mathcal{Z}} \begin{pmatrix} L & l & l' \\ M & m & m' \end{pmatrix} a_{l'm'}^{\mathcal{Z}/\mathcal{Y}}. \quad (99)$$

These expressions differ from those for the one-point estimators by the absence of an extra summation index. If summed over the free index L , the expression for Q_L reduces to a one-point estimator. $Q_L^{\mathcal{X},\mathcal{Y}\mathcal{Z}}[a]$ represents a map as well as $\partial_{lm} Q_L^{\mathcal{X},\mathcal{Y}\mathcal{Z}}[a]$; however, $Q_L^{\mathcal{X},\mathcal{Y}\mathcal{Z}}[a]$ is cubic in input maps a_{lm} s, whereas the derivatives $\partial_{lm} Q_L^{\mathcal{X},\mathcal{Y}\mathcal{Z}}[a]$ are quadratic in input. The expression for the derivative is different when the derivative is taken with respect to the field (e.g. \mathcal{X} in this case) associated with the free indices than when it is taken with respect to a field \mathcal{Y} or \mathcal{Z} , whose indices are summed over.

The skew spectrum can then be written as (the summation convention is assumed for the next two equations):

$$\hat{E}_L^{\mathcal{X},\mathcal{Y}\mathcal{Z}}[a] = [N^{-1}]_{LL'} \left\{ Q_{L'}^{\mathcal{X},\mathcal{Y}\mathcal{Z}}[C^{-1}a] - \sum_S [C^{-1}a]_{lm}^S \langle \partial_{lm}^S Q_{L'}^{\mathcal{X},\mathcal{Y}\mathcal{Z}}[C^{-1}a'] \rangle_{\text{MC}} \right\}; \quad S \in (\mathcal{X}, \mathcal{Y}, \mathcal{Z}) \quad (100)$$

Here $\langle \rangle_{\text{MC}}$ denotes the MC averages. The inverse-covariance matrix in the harmonic domain $[C^{\mathcal{X}\mathcal{Y}}]_{l_1 m_1, l_2 m_2} = \langle a_{l_1 m_1}^{\mathcal{X}} a_{l_2 m_2}^{\mathcal{Y}} \rangle^{-1}$ encodes the effects of noise and the mask. For all-sky and in the signal-only limit, it reduces to the usual $[C^{-1}]_{l_1 m_1, l_2 m_2}^{\mathcal{X}\mathcal{Y}} = \frac{1}{D_l^{\mathcal{X}\mathcal{Y}}} \delta_{ll'} \delta_{mm'}$. The normalization of the estimator, which ensures unit response, can be written as

$$N_{LL'} = \frac{1}{6} \sum_{SS'} \left[\langle \{ \partial_{l_1 m_1}^S Q_L[C^{-1}a] \} [\tilde{C}_{l_1 m_1, l_2 m_2}]^{SS'} \{ \partial_{l_2 m_2}^{S'} Q_{L'}[C^{-1}a] \} \rangle \right. \\ \left. - \langle \{ \partial_{l_1 m_1}^S Q_L[C^{-1}a] \} [C_{l_1 m_1, l_2 m_2}^{-1}]^{SS'} \{ \langle \partial_{l_2 m_2}^{S'} Q_{L'}[C^{-1}a] \rangle \} \rangle \right]; \quad Q_L \equiv Q_L^{\mathcal{X},\mathcal{Y}\mathcal{Z}}; \quad S, S' \in \mathcal{X}, \mathcal{Y}, \mathcal{Z}. \quad (101)$$

In the above expression, and in those that follow, we will not explicitly display the superscript on the normalization matrix $N_{LL'}$ and Q_L as they are obvious from the context. Summing over repeated indices is assumed, and the second term ensures subtraction of terms with self-coupling(s). We will be using the following identity in our derivation:

$$C_{l_1 m_1, l_2 m_2}^{\mathcal{X}\mathcal{Y}} \equiv \langle \tilde{a}_{l_1 m_1}^{\mathcal{X}} \tilde{a}_{l_2 m_2}^{\mathcal{Y}} \rangle = \langle [C^{-1}a]_{l_1 m_1}^{\mathcal{X}} [C^{-1}a]_{l_2 m_2}^{\mathcal{Y}} \rangle = \sum_{\mathcal{X}'\mathcal{Y}'} \sum_{l_a m_a} \sum_{l_b m_b} [C^{-1}]_{l_1 m_1, l_a m_a}^{\mathcal{X}\mathcal{X}'} C_{l_a m_a, l_b m_b}^{\mathcal{X}'\mathcal{Y}'} [C^{-1}]_{l_2 m_2, l_b m_b}^{\mathcal{Y}\mathcal{Y}'}. \quad (102)$$

The Fisher matrix, encapsulating the errors and covariances on the E_L , for a general survey associated with a specific form of bispectrum can finally be written as

$$F_{LL'} = \frac{1}{36} \left((1)\alpha_{LL'}^{PP} + (2)\alpha_{LL'}^{PP} + (1)\alpha_{LL'}^{QQ} + (2)\alpha_{LL'}^{QQ} + (3)\alpha_{LL'}^{QQ} + (4)\alpha_{LL'}^{QQ} \right). \quad (103)$$

Using the following expressions, which are extensions of Smith & Zaldarriaga (2006), we find that the Fisher matrix can be written as a sum of two α terms α^{PP} and α^{QQ} . The terms involved α correspond to coupling only of modes that appear in different $3j$ symbols. Self-couplings are represented by the β terms. The subscripts describe the coupling of various l and L indices. The subscript PP corresponds to coupling of free indices, that is, one free index L_1 with another free index L_2 and similar coupling for indices that are summed over, such as l_1 , l_2 , etc. Similarly, for the subscript QQ , the free indices are coupled with summed indices. Couplings are represented by the inverse-covariance matrices in the harmonic domain; for example, $C_{lm, LM}^{-1}$ denotes coupling of mode LM with lm .

$$(1)\alpha_{L_1 L_2}^{PP} = \sum_{M_1, M_2} \sum_{l_1 l'_1 m_1 m'_1} B_{L_1 l_1 l'_1}^{\mathcal{X}\mathcal{Y}\mathcal{Z}} B_{L_2 l_2 l'_2}^{\mathcal{X}\mathcal{Y}\mathcal{Z}} \begin{pmatrix} L_1 & l_1 & l'_1 \\ M_1 & m_1 & m'_1 \end{pmatrix} \begin{pmatrix} L_2 & l_2 & l'_2 \\ M_2 & m_2 & m'_2 \end{pmatrix} [\tilde{C}_{L_1 M_1, L_2 M_2}]^{\mathcal{X}\mathcal{X}} [\tilde{C}_{l_1 m_1, l_2 m_2}]^{\mathcal{Y}\mathcal{Y}} [\tilde{C}_{l'_1 m'_1, l'_2 m'_2}]^{\mathcal{Z}\mathcal{Z}} \\ (1)\alpha_{L_1 L_2}^{QQ} = \sum_{M_1, M_2} \sum_{l_1 l'_1 m_1 m'_1} B_{L_1 l_1 l'_1}^{\mathcal{X}\mathcal{Y}\mathcal{Z}} B_{L_2 l_2 l'_2}^{\mathcal{X}\mathcal{Y}\mathcal{Z}} \begin{pmatrix} L_1 & l_1 & l'_1 \\ M_1 & m_1 & m'_1 \end{pmatrix} \begin{pmatrix} L_2 & l_2 & l'_2 \\ M_2 & m_2 & m'_2 \end{pmatrix} [\tilde{C}_{L_1 M_1, L_2 M_2}]^{\mathcal{X}\mathcal{Y}} [\tilde{C}_{l_1 m_1, l_2 m_2}]^{\mathcal{Y}\mathcal{X}} [\tilde{C}_{l'_1 m'_1, l'_2 m'_2}]^{\mathcal{Z}\mathcal{Z}} \\ \alpha_{L_1 L_2}^{PP} = (L_1 l_1 l'_1)(L_2 l_2 l'_2); \quad \alpha_{L_1 L_2}^{QQ} = (L_1 l_1 l'_1)(L_2 l_2 l'_2). \quad (104)$$

Similar results for $(2)\alpha_{L_1 L_2}^{PP}$ and $(2-4)\alpha_{L_1 L_2}^{QQ}$ can be obtained from permutative reordering of the above results. The ordering of the multipole indices and that of corresponding fields denoted by \mathcal{X} is important. For each different choice of field triplets, we will have a different set of skew spectra associated with the bispectrum. If we choose to have the same triplets for the primed and unprimed fields, then we will recover the Fisher matrix associated with that specific choice. However, if we decide to choose a different set of triplets, then we will have the information about the level of cross-contamination from one type of power spectra to another. Within a specific choice of triplet, for example, TEE , the choice to associate the free index L to a given field type, for example, T or E will generate two different skew spectra from the same

bispectrum B^{TEE} . Results presented above will reduce to those of Smith & Zaldarriaga (2006), when further summations over free indices L_1 and L_2 are introduced to collapse the two-point object to the corresponding one-point quantity. The β terms that denote cross-coupling are not presented here as they do not appear in the final expressions for the Fisher matrix. A detailed analysis of these terms is presented in Munshi & Heavens (2010) and can be extended in a very similar manner. If we sum over LL' , the Fisher matrix reduces to a scalar $F = \sum_{LL'} F_{LL'}$ with, $\alpha_{LL'}^{PP} = \alpha_{LL'}^{QQ} = \alpha$ and $\beta_{LL'}^{PP} = \beta_{LL'}^{QQ} = \beta$, where α , β and F are exactly the same as introduced in Smith & Zaldarriaga (2006) for one-point estimators.

5.1.1 Joint estimation of multiple bispectrum-related power spectra

The estimation technique described above can be generalized to cover the bispectrum-related power spectrum associated with different sets of bispectra (X, Y) , where X and Y can be one of the combinations from the set $\{(TTT), (TTE), (TEE), (EEE)\}^{loc/eq}$. In addition to considering triplets corresponding to a given primordial bispectrum, we can as well consider joint estimation of different initial primordial bispectra, such as local (loc) or equilateral (eq) bispectra:

$$\hat{E}_L^\Gamma[a] = \sum_S [F^{-1}]_{LL'}^{\Gamma\Gamma'} \left\{ Q_L^{\Gamma'}[C^{-1}a] - \sum_{S'} [C^{-1}a]_{lm}^{S'} \left\langle \partial_{lm}^{S'} Q_L^{\Gamma'}[C^{-1}a] \right\rangle_{MC} \right\}; \quad \Gamma, \Gamma' \in (TTT), (TTE), (TEE), (EEE)^{loc/eq}; \quad S \in T, E. \quad (105)$$

The associated Fisher matrix now will consist of sectors $F_{LL'}^{\Gamma\Gamma}$, $F_{LL'}^{\Gamma\Gamma'}$ and $F_{LL'}^{\Gamma'\Gamma'}$. The sectors $\Gamma\Gamma$ and $\Gamma'\Gamma'$ will, in general, be related to errors associated with estimation of bispectra of Γ and Γ' types, whereas the sector $\Gamma\Gamma'$ will correspond to their cross-correlation. Clearly, with a given mixed bispectrum type, it is possible to have different estimators by associating a specific type of field T or E with the index which is not summed over:

$$F_{LL'}^{\Gamma\Gamma'} = \left\{ \frac{2}{36} [\alpha_{LL'}^{PP} + \dots]^{\Gamma\Gamma'} + \frac{4}{36} [\alpha_{LL'}^{QQ} + \dots]^{\Gamma\Gamma'} \right\}. \quad (106)$$

Here, the dots represent contribution from other terms represented by α , which are obtained from permutation of various indices. We have introduced the following notation above:

$${}_1[\alpha_{LL'}^{PP}]^{\Gamma\Gamma'} = \sum_{MM'} \sum_{l_1 l_1' m_1 m_1'} B_{Ll_1 l_1'}^\Gamma B_{L'l_2 l_2'}^{\Gamma'} \begin{pmatrix} L & l_1 & l_1' \\ M & m_1 & m_1' \end{pmatrix} \begin{pmatrix} L' & l_2 & l_2' \\ M' & m_2 & m_2' \end{pmatrix} [\tilde{C}_{LM, L'M'}]^{\mathcal{X}\mathcal{X}'} [\tilde{C}_{l_1 m_1, l_2 m_2}]^{\mathcal{Y}\mathcal{Y}'} [\tilde{C}_{l_1' m_1', l_2' m_2'}]^{\mathcal{Z}\mathcal{Z}'} \quad (107)$$

and a similar expression holds for the other $[\alpha_{LL'}^{PP}]$ terms as well as the $[\alpha_{LL'}^{QQ}]$ terms. We can also use the above formalism to obtain the cross-correlation of a given skew spectrum type from different kinds of primordial bispectra, as well as, say, local type and equilateral types of non-Gaussianity.

5.1.2 All-sky homogeneous noise

The above expressions are very general results for arbitrary sky coverage due to a specific scanning strategy. Our approach can deal with complications resulting from partial sky coverage and inhomogeneous Gaussian noise. Any residual non-Gaussian noise will have to be subtracted out and will need more elaborate analysis of variance estimation.

If we now take the limiting case, when we have all-sky coverage and homogeneous noise, we can recover analytical results, which are useful for comparing various planned and ongoing surveys. In the all-sky limit, the covariance matrices are determined entirely by signal and noise power spectra. To simplify the general expressions derived so far for the case of all-sky coverage and uniform noise, we will use the following expression:

$$C_{l_1 m_1, l_2 m_2}^{\mathcal{X}\mathcal{Y}} \equiv [C^{-1}]_{l_1 l_2} \delta_{l_1 l_2} \delta_{m_1 m_2} = \begin{pmatrix} 1/d_{l_1}^{TT} & 1/d_{l_1}^{TE} \\ 1/d_{l_1}^{TE} & 1/d_{l_1}^{EE} \end{pmatrix} \delta_{l_1 l_2} \delta_{m_1 m_2}. \quad (108)$$

We recover the following expression for the case of temperature:

$$F_{LL'}^{T,TT} = \frac{1}{36} \left\{ 2\delta_{LL'} \sum_{ll'} \frac{[B_{ll'}^{TTT}]^2}{d_L^T d_{l'}^T d_{l'}^T} + 4 \sum_l \frac{[B_{ll'}^{TTT}]^2}{d_l^T d_l^T d_{l'}^T} \right\}. \quad (109)$$

If we assume that there is no correlation between the temperature and E-type polarization, then $d_l^T = C_l^T$, which reduces to the temperature-only result. Notice that in this case, the corresponding α^{PP} and α^{QQ} functions become degenerate. Expressions for the case of an estimation error of $E_{LL'}^{T,EE}$, $E_{LL'}^{E,TE}$ can be obtained using the following expressions for the related Fisher matrices:

$$F_{LL'}^{T,EE} = \frac{1}{36} \left\{ 2\delta_{LL'} \sum_{ll'} \frac{[B_{ll'}^{TEE}]^2}{d_L^T d_l^E d_{l'}^E} + 4 \sum_l \frac{[B_{ll'}^{TEE}]^2}{d_l^X d_L^X d_{l'}^E} \right\} \quad (110)$$

$$F_{LL'}^{E,TE} = \frac{1}{36} \left\{ \delta_{LL'} \sum_{ll'} [B_{ll'}^{ETE}]^2 \left(\frac{1}{d_L^E d_l^T d_{l'}^E} + \frac{1}{d_L^E d_l^X d_{l'}^X} \right) + \sum_l [B_{ll'}^{ETE}]^2 \left(\frac{1}{d_L^X d_L^X d_l^E} + \frac{1}{d_L^E d_L^E d_l^T} + \frac{1}{d_L^X d_L^X d_l^X} + \frac{1}{d_L^E d_L^E d_l^E} \right) \right\}. \quad (111)$$

The Fisher matrices for $F_{LL'}^{E,TT}$ and $F_{LL'}^{E,EE}$ can also be constructed in a similar manner.

Using a specific form for the bispectrum $b_{l_1 l_2 l_3}^{\text{loc}}$, such as the local model, the Fisher matrix elements can be further expressed in terms of the transfer functions $\alpha^{\mathcal{X}}$ and $\beta^{\mathcal{Y}}$ and the associated power spectra $C_l^{\mathcal{X}\mathcal{Y}}$ using the definitions of ${}_i\alpha^{PP}$ and ${}_i\alpha^{QQ}$ introduced before:

$${}_i[\alpha_{LL'}^{PP}]^{\Gamma\Gamma} = \frac{f_{\text{NL}}^2}{4\pi} (2L+1)(2L'+1) \sum_l (2l+1) \begin{pmatrix} L & L' & l \\ 0 & 0 & 0 \end{pmatrix}^2 \frac{1}{d_L^{\mathcal{X}} d_{L'}^{\mathcal{Y}} d_l^{\mathcal{Z}}} \times \left\{ \int r^2 dr (\alpha_L^{\mathcal{X}}(r) \beta_{L'}^{\mathcal{Y}}(r) \beta_l^{\mathcal{Z}}(r) + \alpha_{L'}^{\mathcal{Y}}(r) \beta_L^{\mathcal{X}}(r) \beta_l^{\mathcal{Z}}(r) + \alpha_l^{\mathcal{Z}}(r) \beta_L^{\mathcal{X}}(r) \beta_{L'}^{\mathcal{Y}}(r)) \right\}^2; \quad \Gamma = \mathcal{X}\mathcal{Y}\mathcal{Z} \quad (112)$$

$${}_i[\alpha_{LL'}^{QQ}]^{\Gamma\Gamma} = \delta_{LL'} \frac{f_{\text{NL}}^2}{4\pi} (2L+1) \sum_{l'} (2l+1)(2l'+1) \begin{pmatrix} L & l & l' \\ 0 & 0 & 0 \end{pmatrix}^2 \frac{1}{d_L^{\mathcal{X}} d_l^{\mathcal{Y}} d_{l'}^{\mathcal{Z}}} \times \left\{ \int r^2 dr (\alpha_L^{\mathcal{X}}(r) \beta_l^{\mathcal{Y}}(r) \beta_{l'}^{\mathcal{Z}}(r) + \alpha_l^{\mathcal{Y}}(r) \beta_{l'}^{\mathcal{Z}}(r) \beta_L^{\mathcal{X}}(r) + \alpha_{l'}^{\mathcal{Z}}(r) \beta_L^{\mathcal{X}}(r) \beta_l^{\mathcal{Y}}(r)) \right\}^2; \quad \Gamma = \mathcal{X}\mathcal{Y}\mathcal{Z}. \quad (113)$$

The power spectra C_l appearing in the denominator take contributions from both the pure signal (i.e. the CMB) and the detector noise. It is possible to bin the estimates in sufficiently large bins that these are practically uncorrelated estimates for an experiment, such as *Planck*, with very high sky coverage. A joint analysis will combine the results from all possible estimators. The cross-correlation among various estimators (characterized by different choices of \mathcal{X} , \mathcal{Y} and \mathcal{Z}) can be computed following the same techniques. A detailed analysis of the singularity structure of the error-covariance matrix will be presented elsewhere.

5.2 Power spectra related to trispectra

Extending our analysis to the case of four-point correlation functions involving both temperature and polarization data, we will next consider the case of one-point and two-point estimators, which are related to the mixed trispectra.

5.2.1 One-point estimators

We will use an inverse-variance weighting for harmonics recovered from the sky. The covariance matrix, expressed in the harmonic domain, $\langle a_{lm}^{\mathcal{U}} a_{l'm'}^{\mathcal{V}} \rangle = [C^{-1}]_{lm, l'm'}^{\mathcal{U}\mathcal{V}}$ is used to filter out modes recovered directly from the sky a_{lm} . We use these harmonics to construct optimal estimators. For all-sky coverage and homogeneous noise, we can recover the results derived in the previous section. We start by keeping in mind that the trispectrum can be expressed in terms of the harmonic transforms a_{lm} , which can either be temperature multipoles or polarization multipoles:

$$T_{\mathcal{W}_{lc} \mathcal{X}_{ld}}^{\mathcal{U}_{la} \mathcal{V}_{lb}} = (2l+1) \sum_{m_i} \sum_M (-1)^M \begin{pmatrix} l_a & l_b & L \\ m_a & m_b & M \end{pmatrix} \begin{pmatrix} l_c & l_d & L \\ m_c & m_d & -M \end{pmatrix} a_{l_a m_a}^{\mathcal{U}} \dots a_{l_d m_d}^{\mathcal{X}} \quad (i \in a, b, c, d), (\mathcal{U}, \mathcal{V}, \mathcal{W}, \mathcal{X}) \in T, E. \quad (114)$$

Based on this expression, we can devise a one-point estimator. In the following discussion, the relevant harmonics can be based on partial sky coverage:

$$Q^{\mathcal{U}\mathcal{V}\mathcal{W}\mathcal{X}}[a] = \frac{1}{4!} \sum_{LM} (-1)^M \sum_{l_i m_i} \Delta(l_i; L) T_{\mathcal{W}_{lc} \mathcal{X}_{ld}}^{\mathcal{U}_{la} \mathcal{V}_{lb}} \begin{pmatrix} l_a & l_b & L \\ m_a & m_b & M \end{pmatrix} \begin{pmatrix} l_c & l_d & L \\ m_c & m_d & -M \end{pmatrix} a_{l_a m_a}^{\mathcal{U}} \dots a_{l_d m_d}^{\mathcal{X}}. \quad (115)$$

The term $\Delta(l_i; L)$ is introduced here to avoid contributions from Gaussian or disconnected contributions: $\Delta(l_i; L)$ vanishes, if any pair of l_i becomes equal or $L = 0$, which effectively reduces the trispectra to a product of two power spectra (i.e. disconnected Gaussian pieces). Its value is unity for the connected terms. We will also need the first-order and second-order derivatives with respect to the input harmonics. The linear terms are proportional to the first derivatives, and the quadratic terms are proportional to second derivatives, of the function $Q[a]$, which is quartic in the input harmonics:

$$\partial_{lm}^{\mathcal{U}} Q^{\mathcal{U}\mathcal{V}\mathcal{W}\mathcal{X}}[a] = \frac{1}{4!} \sum_{LM} (-1)^M \sum_{l_i m_i} \Delta(l_i; L) T_{\mathcal{W}_{lc} \mathcal{X}_{ld}}^{\mathcal{U}_{la} \mathcal{V}_{lb}} \begin{pmatrix} l & l_a & L \\ m & m_a & M \end{pmatrix} \begin{pmatrix} l_b & l_c & L \\ m_b & m_c & -M \end{pmatrix} a_{l_a m_a}^{\mathcal{U}} a_{l_b m_b}^{\mathcal{V}} a_{l_c m_c}^{\mathcal{W}} a_{l_d m_d}^{\mathcal{X}}. \quad (116)$$

The first-order derivative term, such as $\partial_{lm}^{\mathcal{U}} Q^{\mathcal{U}\mathcal{V}\mathcal{W}\mathcal{X}}[a]$, is cubic in input maps and the second-order derivative is quadratic in input maps (in terms of harmonics). However, unlike the estimator itself, $Q^{\mathcal{U}\mathcal{V}\mathcal{W}\mathcal{X}}[a]$, which is simply a number, these objects represent maps constructed from harmonics of the observed maps. The quadratic terms contribute only to disconnected parts and hence will not be considered. The optimal estimator for the one-point cumulant can therefore be written as follows. This is optimal in the presence of partial sky coverage and most general inhomogeneous noise:

$$E^{\mathcal{U}\mathcal{V}\mathcal{W}\mathcal{X}}[a] = \frac{1}{N} \left\{ Q^{\mathcal{U}\mathcal{V}\mathcal{W}\mathcal{X}}[C^{-1}a] - \sum_{S, lm} [C^{-1}a]_{lm}^S \langle \partial_{lm}^S Q^{\mathcal{U}\mathcal{V}\mathcal{W}\mathcal{X}}[C^{-1}a] \rangle \right\}; \quad S \in (\mathcal{U}, \mathcal{V}, \mathcal{W}, \mathcal{X}). \quad (117)$$

The terms, which are subtracted out, can be linear or quadratic in input harmonics. The linear term is similar to the one, which is used for bispectrum estimation, whereas the quadratic terms correspond to the disconnected contributions and will vanish identically as we have

designed our estimators in such a way that it will not take any contribution from disconnected Gaussian terms. The Fisher matrix reduces to a number, which we have used for normalization. The direct summation over various harmonics as described above can be expensive computationally and determines to what resolution the numerical calculation can be performed. The input $[C^{-1}a]$ denote the entire set of inverse variance weighted harmonics for the Q and ∂Q . It is interesting to note that modes after inverse-variance weighting are no longer pure and are linear combinations of temperature and E-type polarization modes. This is true for the case of estimators too. A given estimator $F^{\mathcal{UV}\mathcal{W}\mathcal{X}}$ though corresponds to a specific choice of trispectrum takes contributions from modes, which are themselves linear combinations of pure mode types:

$$F^{\mathcal{UV}\mathcal{W}\mathcal{X}} = \frac{1}{N} = \left(\frac{1}{4!}\right)^2 \sum_{\mathcal{U}'\mathcal{V}'\mathcal{W}'\mathcal{X}'} \sum_{LM} \sum_{L'M'} \sum_{(all\ell m)} \sum_{(all\ell' m')} (-1)^M (-1)^{M'} \Delta(l_i; L) \Delta(l'_i; L') T_{\mathcal{W}\ell_c \mathcal{X}\ell_d}^{\mathcal{U}_a \mathcal{V}_{l_b}}(L) T_{\mathcal{W}\ell'_c \mathcal{X}\ell'_d}^{\mathcal{U}'_a \mathcal{V}'_{l'_b}}(L') \\ \times \begin{pmatrix} l_a & l_b & L \\ m_a & m_b & M \end{pmatrix} \begin{pmatrix} l_c & l_d & L \\ m_c & m_d & -M \end{pmatrix} \begin{pmatrix} l'_a & l'_b & L' \\ m'_a & m'_b & M' \end{pmatrix} \begin{pmatrix} l'_c & l'_d & L' \\ m'_c & m'_d & -M' \end{pmatrix} \\ \times \left\{ [\tilde{C}_{l_a m_a, l'_a m'_a}]^{\mathcal{U}\mathcal{U}'} \dots [\tilde{C}_{l_d m_d, l'_d m'_d}]^{\mathcal{W}\mathcal{W}'} + \text{cyclic permutation} \right\}. \quad (118)$$

The cyclic permutations in these terms will include covariances involving all-possible permutations of the four fields involved in the construction of the mixed trispectrum and the related power spectra. The ensemble average of this one-point estimator will be a linear combination of parameters f_{NL}^2 and g_{NL} . Estimators constructed at the level of three-point cumulants (Smith & Zaldarriaga 2006; Munshi & Heavens 2010) can be used jointly with this estimator to put independent constraints separately on f_{NL} and g_{NL} . As discussed before, while the one-point estimator has the advantage of higher S/N, such estimators are not immune to contributions from an unknown component which may not have cosmological origin, such as inadequate foreground separation. The study of these power spectra associated with bispectra or trispectra can be useful in this direction. Note that these direct estimators are computationally expensive due to the inversion and multiplication of large matrices, but can be implemented in low-resolution studies, where primordial signals may be less contaminated by foreground contributions or secondaries.

Combining all possible choices of mixed trispectra, it is possible to introduce one single number which represents the entire information content regarding the trispectrum from temperature and E-type polarization in the absence of B modes. The corresponding estimators and the Fisher matrix takes the following form:

$$E^{(4)} = \sum_{\mathcal{UV}\mathcal{W}\mathcal{X}} E^{\mathcal{UV}\mathcal{W}\mathcal{X}}; \quad F^{(4)} = \sum_{\mathcal{UV}\mathcal{W}\mathcal{X}} F^{\mathcal{UV}\mathcal{W}\mathcal{X}}. \quad (119)$$

The choice of estimators is related to the level of compromise one is willing to made to increase the S/N at the expense of losing the crucial power to distinguish contributions from various contributions. Clearly, it is also possible to design estimators by fixing a subset of all available indices representing the choice of T or E .

5.2.2 Two-point estimators

Generalizing the above expressions for the case of the power spectrum associated with trispectra, we introduce two power spectra, which we have discussed in the previous section in the context of construction of nearly-optimal estimators. The information content in these power spectra is optimal, and when summed over L , we can recover the results of one-point estimators:

$$Q_L^{(\mathcal{UV}, \mathcal{W}\mathcal{X})}[a] = \frac{1}{4!} \sum_M (-1)^M \sum_{l_i m_i} T_{\mathcal{W}\ell_c \mathcal{X}\ell_d}^{\mathcal{U}_a \mathcal{V}_{l_b}}(L) \begin{pmatrix} l_a & l_b & L \\ m_a & m_b & M \end{pmatrix} \begin{pmatrix} l_c & l_d & L \\ m_c & m_d & -M \end{pmatrix} a_{l_a m_a}^{\mathcal{U}} \dots a_{l_d m_d}^{\mathcal{X}}. \quad (120)$$

The derivatives at the first order and second order are as a series of maps (for each L) constructed from the harmonics of the observed sky. These are used in the construction of linear and quadratic terms. We have retained the overall normalization factor $\frac{1}{4!}$ so that our estimator reduces to the temperature-only estimator introduced in Munshi et al. (2009):

$$\partial_{lm}^{\mathcal{U}} Q_L^{(\mathcal{UV}, \mathcal{W}\mathcal{X})}[a] = \frac{1}{4!} \sum_T (-1)^M \sum_{l_i m_i} \Delta(l_i; L) T_{\mathcal{W}\ell_c \mathcal{X}\ell_d}^{\mathcal{U}_a \mathcal{V}_{l_b}}(L) \begin{pmatrix} l & l_a & L \\ m & m_b & M \end{pmatrix} \begin{pmatrix} l_b & l_c & L \\ m_b & m_c & -M \end{pmatrix} a_{l_a m_a}^{\mathcal{U}} \dots a_{l_c m_c}^{\mathcal{X}}. \quad (121)$$

We can construct the other estimator in a similar manner. To start with, we define the function $Q_L^{(\mathcal{U}, \mathcal{V}\mathcal{W}\mathcal{X})}[a]$ and construct its first and second derivatives. These are eventually used for construction of the estimator $E_L^{(\mathcal{U}, \mathcal{V}\mathcal{W}\mathcal{X})}[a]$. As we have seen, both these estimators can be collapsed to a one-point estimator $Q^{\mathcal{UV}\mathcal{W}\mathcal{X}}[a]$. As before, the variable a here denotes input harmonics $a_{lm}^{\mathcal{U}}$ recovered from the noisy observed sky:

$$Q_L^{(\mathcal{U}, \mathcal{V}\mathcal{W}\mathcal{X})}[a] = \frac{1}{4!} \sum_M \sum_{ST} (-1)^T a_{LM}^{\mathcal{U}} \sum_{l_i m_i} \Delta(l_i; L; T) T_{\mathcal{W}\ell_c \mathcal{X}\ell_d}^{\mathcal{U}_a \mathcal{V}_{l_b}}(T) \begin{pmatrix} L & l_b & S \\ M & m_b & T \end{pmatrix} \begin{pmatrix} l_c & l_d & S \\ m_c & m_d & -T \end{pmatrix} a_{l_b m_b}^{\mathcal{V}} \dots a_{l_d m_d}^{\mathcal{X}}. \quad (122)$$

The derivative terms will have two contributing terms corresponding to the derivative with respect to the free index $\{LM\}$ and the terms where indices are summed over, for example, $\{lm\}$, which is very similar to the results for the bispectrum analysis with the estimator $Q_L^{(\mathcal{X}\mathcal{Y}, \mathcal{Z})}[a]$. One major difference that needs to be taken into account is the subtraction of the Gaussian contribution. The function $\Delta(l_i, L)$ takes into

account this subtraction:

$$\partial_{lm}^{\mathcal{U}} \mathcal{Q}_L^{(\mathcal{U}, \mathcal{V}\mathcal{W}\mathcal{X})}[a] = \delta_{lL} \sum_{ST} \sum_{l_i m_i} \Delta(l_i, L; T) T_{\mathcal{W}l_3 \mathcal{X}l_4}^{\mathcal{U}l_1 \mathcal{V}l_2}(T) \begin{pmatrix} l & l_b & S \\ m & m_b & T \end{pmatrix} \begin{pmatrix} l_c & l_d & S \\ m_c & m_d & -T \end{pmatrix} a_{l_b m_b}^{\mathcal{V}} \dots a_{l_d m_d}^{\mathcal{W}} \quad (123)$$

$$\partial_{lm}^{\mathcal{X}} \mathcal{Q}_L^{(\mathcal{U}, \mathcal{V}\mathcal{W}\mathcal{X})}[a] = \sum_M \sum_{l_i m_i} a_{LM}^{\mathcal{U}} \sum_T \Delta(l_i, L; T) T_{\mathcal{W}l_3 \mathcal{X}l_4}^{\mathcal{U}l_1 \mathcal{V}l_2}(S) \begin{pmatrix} L & l & S \\ M & m & T \end{pmatrix} \begin{pmatrix} l_b & l_c & S \\ m_b & m_c & -T \end{pmatrix} a_{l_b m_b}^{\mathcal{V}} a_{l_c m_c}^{\mathcal{W}}. \quad (124)$$

Using these derivatives, we can construct the estimators $E_L^{(\mathcal{U}, \mathcal{V}\mathcal{W}\mathcal{X})}$ and $E_L^{(\mathcal{U}\mathcal{V}, \mathcal{W}\mathcal{X})}$:

$$E_L^{(\mathcal{U}, \mathcal{V}\mathcal{W}\mathcal{X})} = N_{LL'}^{-1} \left\{ \mathcal{Q}_{L'}^{(\mathcal{U}, \mathcal{V}\mathcal{W}\mathcal{X})}[C^{-1}a] - \sum_S [C^{-1}a]_{lm}^S \langle \partial_{lm}^S \mathcal{Q}_{L'}^{(\mathcal{U}, \mathcal{V}\mathcal{W}\mathcal{X})}[C^{-1}a] \rangle \right\}; \quad S \in \mathcal{U}, \mathcal{V}, \mathcal{W}, \mathcal{X} \quad (125)$$

$$E_L^{(\mathcal{U}\mathcal{V}, \mathcal{W}\mathcal{X})} = N_{LL'}^{-1} \left\{ \mathcal{Q}_{L'}^{(\mathcal{U}\mathcal{V}, \mathcal{W}\mathcal{X})}[C^{-1}a] - \sum_S [C^{-1}a]_{lm}^S \langle \partial_{lm}^S \mathcal{Q}_{L'}^{(\mathcal{U}\mathcal{V}, \mathcal{W}\mathcal{X})}[C^{-1}a] \rangle \right\}; \quad S \in \mathcal{U}, \mathcal{V}, \mathcal{W}, \mathcal{X}, \quad (126)$$

where summation over L' is implied. The quadratic terms will vanish, as they contribute only to the disconnected part. The normalization constants are the Fisher matrix elements $F_{LL'}$, which can be expressed in terms of the target trispectrum $T_{l_3 l_4}^{l_1 l_2}(L)$ and inverse-covariance matrices C^{-1} used for the construction of these estimators. The Fisher matrix for the estimator $E_L^{(\mathcal{U}, \mathcal{V}\mathcal{W}\mathcal{X})}$, that is, $F_{LL'}^{(\mathcal{U}, \mathcal{V}\mathcal{W}\mathcal{X})}$, can be expressed as

$$\begin{aligned} [N^{-1}]_{LL'} = F_{LL'}^{(\mathcal{U}, \mathcal{V}\mathcal{W}\mathcal{X})} &= \left(\frac{1}{4!} \right)^2 \sum_{ST, S'T'} \sum_{(alllm, l'm')} (-1)^M (-1)^{M'} \left[T_{\mathcal{W}l_c \mathcal{X}l_d}^{\mathcal{U}l_a \mathcal{V}l_b}(S) \right] \left[T_{\mathcal{W}'l'_c \mathcal{X}'l'_d}^{\mathcal{U}'l'_a \mathcal{V}'l'_b}(S') \right] \Delta(l_i; L) \Delta(l'_i; L') \\ &\times \begin{pmatrix} l_a & l_b & S \\ m_a & m_b & T \end{pmatrix} \begin{pmatrix} L & l_d & S \\ M & m_d & -T \end{pmatrix} \begin{pmatrix} l'_a & l'_b & S' \\ m'_a & m'_b & T' \end{pmatrix} \begin{pmatrix} L' & l'_d & S' \\ M' & m'_d & -T' \end{pmatrix} \\ &\times \left\{ [\tilde{C}_{LM, L'M'}]^{\mathcal{U}\mathcal{U}'} [\tilde{C}_{l_a m_a, l'_a m'_a}]^{\mathcal{V}\mathcal{V}'} [\tilde{C}_{l_b m_b, l'_b m'_b}]^{\mathcal{W}\mathcal{W}'} [\tilde{C}_{l_c m_c, l'_c m'_c}]^{\mathcal{X}\mathcal{X}'} + \dots \right. \\ &\left. + [\tilde{C}_{LM, L'M'}]^{\mathcal{U}\mathcal{V}'} [\tilde{C}_{l_a m_a, L'M'}]^{\mathcal{V}\mathcal{U}'} [\tilde{C}_{l_b m_b, l'_b m'_b}]^{\mathcal{W}\mathcal{W}'} [\tilde{C}_{l_c m_c, l'_c m'_c}]^{\mathcal{X}\mathcal{X}'} + \dots \right\}. \quad (127) \end{aligned}$$

The first set of terms can be recovered from the first term by permuting the multipole indices, while still keeping the coupling of the free indices LL' intact. Similarly, the second set of terms represented by \dots can be recovered from the second terms, but considering only coupling between free indices and the one that are summed over. There will be a total of six terms of the first type and 18 of the second type. Similarly, for the other estimator $E_L^{(\mathcal{U}\mathcal{V}, \mathcal{W}\mathcal{X})}$, the Fisher matrix $F_{LL'}^{(\mathcal{U}\mathcal{V}, \mathcal{W}\mathcal{X})}$ can be written as a function of the associated trispectrum and the covariance matrix of various modes. For further simplification of these expressions, we need to make simplifying assumptions for a specific type of trispectra (see Munshi & Heavens 2010 for more details for such simplifications in the bispectrum):

$$\begin{aligned} [N^{-1}]_{LL'} = F_{LL'}^{(\mathcal{U}\mathcal{V}, \mathcal{W}\mathcal{X})} &= \left(\frac{1}{4!} \right)^2 \sum_M \sum_{M'} \sum_{(alllm)} \sum_{(alll'm')} (-1)^M (-1)^{M'} T_{\mathcal{W}l_c \mathcal{X}l_d}^{\mathcal{U}l_a \mathcal{V}l_b}(L) T_{\mathcal{W}'l'_c \mathcal{X}'l'_d}^{\mathcal{U}'l'_a \mathcal{V}'l'_b}(L') \begin{pmatrix} l_a & l_b & L \\ m_a & m_b & M \end{pmatrix} \begin{pmatrix} L & l_d & L \\ M & m_d & -M \end{pmatrix} \\ &\times \begin{pmatrix} l'_a & l'_b & L' \\ m'_a & m'_b & M' \end{pmatrix} \begin{pmatrix} L' & l'_d & L' \\ M' & m'_d & -M' \end{pmatrix} \Delta(l_i; L) \Delta(l'_i; L') \left\{ [\tilde{C}_{l_a m_a, l'_a m'_a}]^{\mathcal{U}\mathcal{U}'} \dots [\tilde{C}_{l_d m_d, l'_d m'_d}]^{\mathcal{X}\mathcal{X}'} + \text{cyc.perm.} \right\} \quad (128) \end{aligned}$$

Knowledge of the sky coverage and the noise characteristics resulting from a specific scanning strategy is needed for modelling of $[C^{-1}]_{l_a m_a, l'_a m'_a}^{\mathcal{U}\mathcal{U}'}$. We will discuss the impact of inaccurate modelling of the covariance matrix in the next section. The direct summation we have used for the construction of the Fisher matrix may not be feasible except for low-resolution studies. However, a hybrid method may be employed to combine the estimates from low-resolution maps using the exact method with estimates from higher resolution maps using other faster but suboptimal techniques described in previous section. In certain situations, when the data are noise-dominated, further approximations can be made to simplify the implementation; a more detailed discussion will be presented elsewhere. It is possible to sum over all possible trispectra to recover the entire information content:

$$E_l^{(1,3)} = \sum_{\mathcal{U}\mathcal{V}\mathcal{W}\mathcal{X}} E_l^{(\mathcal{U}, \mathcal{V}\mathcal{W}\mathcal{X})}; \quad F_{LL'}^{(1,3)} = \sum_{\mathcal{U}\mathcal{V}\mathcal{W}\mathcal{X}} F_{LL'}^{(\mathcal{U}, \mathcal{V}\mathcal{W}\mathcal{X})}; \quad E_l^{(2,2)} = \sum_{\mathcal{U}\mathcal{V}, \mathcal{W}\mathcal{X}} E_l^{(\mathcal{U}\mathcal{V}, \mathcal{W}\mathcal{X})}; \quad F_{LL'}^{(1,3)} = \sum_{\mathcal{U}\mathcal{V}\mathcal{W}\mathcal{X}} F_{LL'}^{(\mathcal{U}, \mathcal{V}\mathcal{W}\mathcal{X})}. \quad (129)$$

Summing over the free indices, we recover the one-point estimators and the corresponding Fisher matrices:

$$E^{(4)} = \sum_l E_l^{(1,3)} = \sum_l E_l^{(2,2)}; \quad F^{(4)} = \sum_{LL'} F_{LL'}^{(2,2)} = \sum_{LL'} F_{LL'}^{(1,3)}. \quad (130)$$

So far we have assumed that the covariance matrix can be modelled accurately. In the next section, we will discuss the impact of not knowing the covariance matrix accurately. We will show that though the estimators still remain unbiased, but they no longer remain optimal.

5.2.3 Approximation to exact C^{-1} weighting and non-optimal weighting

If the covariance matrix is not accurately known, which is most often the case due to the lack of exact beam or noise characteristics, as well as due to limitations on computer resources to model it to high accuracy, it can be approximated. An approximation R of C^{-1} then acts as a regularization method. The corresponding generic estimator can then be expressed as

$$\hat{E}_L^Z[a] = \sum_{L'} [F^{-1}]_{LL'} \left\{ Q_L^Z[Ra] - \sum_S [Ra]_{lm}^S \langle \partial_{lm}^S Q_L^Z[Ra] \rangle \right\}; \quad Z \in \{(\mathcal{UV}, \mathcal{WX}), (\mathcal{U}, \mathcal{VWX})\}; \quad S \in \mathcal{U}, \mathcal{V}, \mathcal{W}, \mathcal{X}. \quad (131)$$

As before we have assumed sums over repeated indices and $\langle \cdot \rangle$ denote MC averages. As is evident from the notation, the estimator above can be of type $E_L^{(\mathcal{UV}, \mathcal{VWX})}$ or $E_L^{(\mathcal{UV}, \mathcal{WX})}$. For the collapsed case, $E_L^{(4)}$ can also be handled in a very similar manner:

$$\hat{E}^Z[a] = \sum_L E_L^Z = \sum_{LL'} [F^{-1}]_{LL'} \left\{ Q_L^Z[Ra] - [Ra]_{lm}^S \langle \partial_{lm}^S Q_L^Z[Ra] \rangle \right\} \quad Z \in \{(\mathcal{UV}, \mathcal{WX}), (\mathcal{U}, \mathcal{VWX})\}; \quad S \in \mathcal{U}, \mathcal{V}, \mathcal{W}, \mathcal{X}. \quad (132)$$

We will drop the superscript Z for simplicity, but any conclusion drawn below will be valid for both specific cases, that is, $Z \in \{(\mathcal{UV}, \mathcal{WX}), (\mathcal{U}, \mathcal{VWX})\}$. The normalization constant, which also acts as an inverse of associated Fisher matrix $F_{LL'}$, can be written as

$$F_{LL'} = \langle (\hat{E}_L)(\hat{E}_{L'}) \rangle - \langle (\hat{E}_L) \rangle \langle (\hat{E}_{L'}) \rangle = \frac{1}{4} \sum_{SS'} \left\{ \left\langle \partial_{lm}^S Q_L[Ra] [C^{-1}]_{lm,l'm'}^{SS'} \partial_{l'm'}^{S'} Q_{L'}[Ra] \right\rangle - \langle \partial_{lm}^S Q_L[Ra] \rangle [C^{-1}]_{lm,l'm'}^{SS'} \langle \partial_{l'm'}^{S'} Q_{L'}[Ra] \rangle \right\}; \quad S, S' \in (\mathcal{U}, \mathcal{V}, \mathcal{W}, \mathcal{X}). \quad (133)$$

The construction of $F_{LL'}$ is equivalent to the calculation presented for the case of $R = C^{-1}$. Similarly, for the one-point estimator, we can write $F^R = \sum_{LL'} F_{LL'}^R$. The optimal weighting can be replaced by arbitrary weighting. As a special case, we can also use no weighting at all $R = I$. This reduces the cost of the estimator drastically. Although the estimator still remains unbiased, the scatter, however, increases as the estimator is no longer optimal. Use of arbitrary weights makes the estimator equivalent to a PCL estimator discussed before. In certain circumstances, the use of a fast method can be very useful before applying more robust and optimal techniques.

5.2.4 Joint estimation of multiple mixed trispectra

It may be of interest to estimate several trispectra jointly. The different sources of trispectra can be of all primordial type, such as from ‘adiabatic’ and ‘isothermal’ perturbations. Such an estimation can explore the joint error budget on parameters involved from the same data set. In such scenarios, it is indeed important to construct a joint Fisher matrix which will take the form

$$\hat{E}_L^\Gamma[a] = \sum_{\Gamma\Gamma'} [F^{-1}]_{LL'}^{\Gamma\Gamma'} \hat{E}_{L'}^{\Gamma'}[a]; \quad \Gamma, \Gamma' \in \text{Adiabatic, Isothermal}. \quad (134)$$

The estimator $\hat{E}_L^X[a]$ is generic and it could be either $E^{(3,1)}$ or $E^{(2,2)}$. Here, X and Y corresponds to different trispectra of type X and Y ; these could be, for example, primordial trispectra from various inflationary scenarios. It is possible of course to do a joint estimation of primary and secondary trispectra. The off-diagonal blocks of the Fisher matrix will correspond to the cross-talk between various types of bispectra. Indeed, a principal component or generalized eigenmode analysis can be useful in finding how many independent components of such trispectra can be estimated from the data.

The cross-terms in the Fisher matrix elements will be of the following type:

$$\begin{aligned} F_{LL'}^{XY} &= \left(\frac{1}{4!} \right)^2 \sum_{ST, S'T'} \sum_{(alllm, l'm')} (-1)^T (-1)^{T'} \left[T_{\mathcal{W}l_c, \mathcal{X}l_c}^{l_a l_b} (L) \right]^\Gamma \left[T_{\mathcal{W}l'_c, \mathcal{X}l'_c}^{l'_a l'_b} (L') \right]^{\Gamma'} \\ &\times \begin{pmatrix} l_a & l_b & S \\ m_a & m_b & T \end{pmatrix} \begin{pmatrix} L & l_d & S \\ M & m_d & -T \end{pmatrix} \begin{pmatrix} l'_a & l'_b & S' \\ m'_a & m'_b & T' \end{pmatrix} \begin{pmatrix} L' & l'_d & S' \\ M' & m'_d & -T' \end{pmatrix} \\ &\times \left\{ [\tilde{C}_{LM, L'M'}]^{l_a l_b} [\tilde{C}_{l_a m_a, l'_a m'_a}]^{l_b l'_b} [\tilde{C}_{l_b m_b, l'_b m'_b}]^{l_c l'_c} [\tilde{C}_{l_c m_c, l'_c m'_c}]^{l_d l'_d} + \dots \right. \\ &\left. + [\tilde{C}_{LM, l'_a m'_a}]^{l_a l'_a} [\tilde{C}_{l_a m_a, L'M'}]^{l_b l'_b} [\tilde{C}_{l_b m_b, l'_b m'_b}]^{l_c l'_c} [\tilde{C}_{l_c m_c, l'_c m'_c}]^{l_d l'_d} + \dots \right\}. \end{aligned} \quad (135)$$

The expression displayed above is valid only for $E^{(\mathcal{UV}, \mathcal{WX})}$; exactly similar results hold for the other estimator $E^{(\mathcal{U}, \mathcal{VWX})}$. For $X = Y$, we recover the results presented in the previous section for independent estimates. As before, we recover the usual result for a one-point estimator for Q^4 from the Fisher matrix of $Q_L^{(3,1)}$ or $Q_L^{(2,2)}$, with corresponding estimator modified accordingly:

$$F^{\Gamma\Gamma'} = \sum_{\Gamma\Gamma'} F_{LL'}^{\Gamma\Gamma'}; \quad \hat{E}^\Gamma[a] = \sum_{\Gamma\Gamma'} [F^{-1}]^{\Gamma\Gamma'} \hat{E}^{\Gamma'}[a]. \quad (136)$$

A joint estimation can provide clues to cross-contamination from different sources of trispectra. It also provides information about the level of degeneracy involved in such estimates. It is also possible to do joint estimation involving two different types of power spectra associated with trispectra or to include even the power spectrum associated with the bispectrum. The results presented in this section can be generalized to include such cases too.

6 CONCLUSION

The ongoing all-sky survey performed by the *Planck* satellite will complete mapping the CMB sky in unprecedented detail, covering a huge frequency range. It will provide high-resolution temperature and polarization maps, which will provide the cosmological community with the opportunity to constrain available theoretical models with unprecedented accuracy. Recent detection of non-Gaussianity in *WMAP* data has added momentum to non-Gaussianity studies.

The temperature and polarization power spectra carry the bulk of the cosmological information, though many degenerate early universe scenarios can lead to similar power spectra. Higher order multispectra can lift these degeneracies. The higher order spectra are the harmonic transforms of multipoint correlation functions, which contain information that can be difficult to extract using conventional techniques. This is related to their complicated response to the inhomogeneous noise and partial sky coverage. Analysis of the higher order polarization statistics is more complicated not only by relatively low S/N and their spinorial nature, but also because of uncertainties in modelling the polarized foreground. A practical advance is to form collapsed two-point statistics, constructed from higher order correlations, which can be extracted using conventional power-spectrum estimation methods. If the polarization data can be analysed and handled properly, then it can help to further tighten the constraints on parameters describing non-Gaussianity that are achieved by analysis of temperature data alone.

In a recent study, Munshi et al. (2009) studied and developed three different types of estimators, which can be employed to analyse these power spectra associated with higher order statistics, such as a bispectrum or trispectrum for analysis of temperature data. In this work, we include polarization on top of this to further tighten the constraints. The analysis of polarization data makes the analysis bit involved because of the spinorial nature of the data. We start with the MASTER-based approach (Hivon et al. 2002), which is typically employed to estimate PCLs from the masked sky in the presence of noise. These are unbiased estimators, but the associated variances and scatter can be estimated analytically with very few simplifying assumptions. We extend these estimators to study higher order correlation function associated mixed multispectra, such as a bispectrum and a trispectrum, which involve both temperature and polarization. Ignoring the contributions from B polarization makes these estimators much simpler. These estimators can be very useful for testing the simulation pipeline running MC chain in a rather smaller time-scale to spot spurious contributions from foreground or other secondary sources. Generalizing the temperature-only estimators, we develop estimators for $C_l^{(\mathcal{U}\mathcal{V},\mathcal{W})}$ for the skew spectrum (three-point) for specific, but arbitrary choice of $\mathcal{U}, \mathcal{V}, \mathcal{W}, \mathcal{X}$ as well as $C_l^{(\mathcal{U},\mathcal{V}\mathcal{W}\mathcal{X})}$ and $C_l^{(\mathcal{U}\mathcal{V},\mathcal{W}\mathcal{X})}$, which are power spectra of fields related to the specific choice of a mixed trispectrum or kurt spectrum involving temperature and E-type polarization fields.

For our next step, we generalized the estimators employed by Yadav et al. (2007), Yadav & Wandelt (2008) and Yadav et al. (2008) to study the kurt spectrum. These methods are computationally less expensive and can be implemented using an MC pipeline, which involve the generation of three-dimensional maps from the cut-sky harmonics using radial integrations of a target theoretical model bispectrum along the line of sight. The MC generation of three-dimensional maps is the most computationally expensive part and dominates the calculation. Including polarization field increases the computational cost. The technique nevertheless has been used extensively, as it remains highly parallelizable and is near optimal in the presence of homogeneous noise and near all-sky coverage. The corrective terms involve linear and quadratic contributions for the lack of spherical symmetry due to the presence of inhomogeneous noise and partial sky coverage. These terms can be computed using an MC chain for joint temperature and polarization data, but including polarization data requires the ability to handle further complications with an added level of sophistication. We also showed that the radial integral involved at the three-point analysis needs to be extended to incorporate a double integral for the mixed trispectrum. For every choice of the bi- or tri-spectrum involving a specific combination of temperature and polarization fields, related power spectra can always be defined. These can help as a diagnosis for cross-contamination from non-primordial sources in different available frequency channels.

Though the estimators based on the MC analysis based method are very fast, they do not accurately take care of the mode-mode coupling, which are present at least at low resolution. We have developed estimators, which are completely optimal even in the presence of inhomogeneous noise and arbitrary sky coverage (e.g. Smith & Zaldarriaga 2006). These can handle mode-mode coupling more accurately. Extending previous work by Munshi & Heavens (2010), which concentrated only on the skew spectrum, Munshi et al. (2009) showed how to generalize it to the case of power spectrum related to the trispectrum. In this study, we have included polarization in a completely general manner both at the level of the bispectrum and at the level of the trispectrum. This involves finding a fast method to construct and invert the joint covariance matrix $C_{lm'l'm'}$ in multipole space. In most practical circumstances, it is possible only to find an approximation to the exact joint covariance matrix, and to cover this, we present an analysis for an approximate matrix, which can be used instead of C^{-1} . This makes the method marginally suboptimal, but it remains unbiased. The four-point correlation function also takes contributions, which are purely Gaussian in nature. The subtraction of these contributions is again simplified by the use of Gaussian MC-polarized maps with the same power spectrum. A joint Fisher analysis is presented for the construction of the error covariance matrix, allowing joint estimation of trispectrum contributions from various polarized sources, primaries or secondaries. Such a joint estimation gives us fundamental limits on how many sources of non-Gaussianity can be jointly estimated from a specific experimental setup, which scans the sky for temperature as well as for polarization.

At the level of the bispectrum, primordial non-Gaussianity can, for many models, be described by a single parameter f_{NL} . The two degenerate power spectra related to the trispectrum we have studied at the four-point level require two parameters, typically f_{NL} and g_{NL} . Use of the two power spectra will enable us to put separate constraints on f_{NL} and g_{NL} without using information from lower order analysis of the bispectrum, but they can all be used in combination (see Smidt et al. 2010). Clearly, at even higher order, more parameters will be needed to describe various parameters ($f_{\text{NL}}, g_{\text{NL}}, h_{\text{NL}}, \dots$), which will be essential in describing degenerate sets of power spectra associated

Table 1. Error forecast for temperature-only analysis.

l_{\max}	500	1000	1500
$f_{\text{NL}} (Planck)$	16	10	8
$f_{\text{NL}} (EPIC)$	15	7.5	5
$\tau_{\text{NL}} (Planck)$	4350	1640	1550
$\tau_{\text{NL}} (EPIC)$	3700	920	400
$g_{\text{NL}} (Planck)$	1.6^5	1.4×10^5	1.3×10^5
$g_{\text{NL}} (EPIC)$	1.5×10^5	1.1×10^5	6.0×10^4

Table 2. Error forecast for joint temperature and polarization analysis.

l_{\max}	500	1000	1500
$f_{\text{NL}} (Planck)$	8	6	5
$f_{\text{NL}} (EPIC)$	7	5	3
$\tau_{\text{NL}} (Planck)$	1004	390	370
$\tau_{\text{NL}} (EPIC)$	850	220	95
$g_{\text{NL}} (Planck)$	3.8×10^4	3.7×10^4	3.6×10^4
$g_{\text{NL}} (EPIC)$	3.5×10^4	2.6×10^4	1.4×10^4

with multispectra at a specific level. Previous studies concentrated only on temperature data, including information from polarization data can improve the constraints. At present, the polarization data are dominated by noise, but surveys, such as *Planck*, will improve the S/N available in polarization data. Future all-sky high-sensitivity polarization surveys too can further improve the situation and our estimators will be useful for analysis of such data. Numerical implementation of our estimators will be reported elsewhere. We have ignored the presence of B-mode polarization, but our formalism can be extended to take into account the magnetic or B-type polarization.

Tables 1 and 2 show our 1σ error forecasts for parameters f_{NL} , τ_{NL} and g_{NL} . We have taken two different experiments for this purpose, ongoing *Planck* surveyor as well as the proposed EPIC mission (cosmic variance limited case, see e.g. Bock et al. 2009). We have quoted our results for three different values of $l_{\max} = 500, 1000$ and 1500 .

The analytical results presented here can also be useful in the context of study of shear data from weak-lensing surveys. We plan to present our results elsewhere (Munshi et al. 2010).

ACKNOWLEDGMENTS

DM acknowledges support from STFC standard grant ST/G002231/1 at the School of Physics and Astronomy at Cardiff University. This work was initiated when DM was supported by a STFC postdoctoral fellowship at the Royal Observatory, Institute for Astronomy, Edinburgh. It is a pleasure to thank Walter Gear for useful exchanges. We also acknowledge many useful discussions with Michele Liguori. AC and JS acknowledge support from NSF AST-0645427 and NASA NNX10AD42G.

REFERENCES

- Acquaviva V., Bartolo N., Matarrese S., Riotto A., 2003, Nucl. Phys. B, 667, 119
 Babich D., 2005, Phys. Rev. D, 72, 043003
 Bartolo N., Matarrese S., Riotto A., 2006, JCAP, 06, 024
 Baumann et al., 2009, preprint (arXiv:0811.3919)
 Bock J. et al., 2009, preprint (arXiv:0906.1188)
 Cabella P., Hansen F. K., Liguori M., Marinucci D., Matarrese S., Moscardini L., Vittorio N., 2006, MNRAS, 369, 819
 Calabrese E. et al., 2009, preprint (arXiv:0907.3229)
 Chen G., Szapudi I., 2006, ApJ, 647, L87
 Chen X., Huang M., Kachru S., Shiu G., 2007a, JCAP, 0701, 002
 Chen X., Easther R., Lim E. A., 2007b, JCAP, 0706:023
 Cooray A., 2001, Phys. Rev. D, 64, 043516
 Cooray A. R., Hu W., 2000, ApJ, 534, 533
 Cooray A., Kesden M., 2003, New Astron., 8, 231
 Cooray A., Li C., Melchiorri A., 2008, Phys. Rev. D, 77, 103506
 Creminelli P., 2003, JCAP, 0310, 003
 Creminelli P., Nicolis A., Senatore L., Tegmark M., Zaldarriaga M., 2006, JCAP, 5, 4
 Creminelli P., Senatore L., Zaldarriaga M., Tegmark M., 2007, JCAP, 3, 5
 Creminelli P., Senatore L., Zaldarriaga M., 2007, JCAP, 3, 19
 Edmonds A. R., 1968, Angular Momentum in Quantum Mechanics, 2nd edn. Princeton Univ. Press, Princeton, NJ
 Falk T., Madden R., Olive K. A., Srednicki M., 1993, Phys. Lett. B, 318, 354

- Gangui A., Lucchin F., Matarrese S., Mollerach S., 1994, *ApJ*, 430, 447
- Gupta S., Berera A., Heavens A. F., Matarrese S., 2002, *Phys. Rev. D*, 66, 043510
- Heavens A. F., 1998, *MNRAS*, 299, 805
- Hikage C., Munshi D., Heavens A., Coles P., 2010, *MNRAS*, 404, 1505
- Hivon E., Górski K. M., Netterfield C. B., Crill B. P., Prunet S., Hansen F., 2002, *ApJ*, 567, 2
- Hu W., 2000, *Phys. Rev. D*, 62, 043007
- Hu W., Okamoto T., 2002, *ApJ*, 574, 566
- Kogo N., Komatsu E., 2006, *Phys. Rev. D*, 73, 083007
- Komatsu E., Spergel D. N., 2001, *Phys. Rev. D*, 63, 3002
- Komatsu E., Wandelt B. D., Spergel D. N., Banday A. J., Górski K. M., 2002, *ApJ*, 566, 19
- Komatsu E. et al., 2003, *ApJS*, 148, 119
- Komatsu E., Spergel D. N., Wandelt B. D., 2005, *ApJ*, 634, 14
- Koyama K., Mizuno S., Vernizzi F., Wands D., 2007, *JCAP*, 0711:024
- Larson D. et al., 2010, preprint (arXiv:1001.4635)
- Liguori M., Yadav A., Hansen F. K., Komatsu E., Matarrese S., Wandelt B., 2007, *Phys. Rev. D*, 76, 105016
- Linde A. D., Mukhanov V. F., 1997, *Phys. Rev. D*, 56, 535
- Lyth D. H., Ungarelli C., Wands D., 2003, *Phys. Rev. D*, 67, 023503
- Maldacena J. M., 2003, *JHEP*, 05, 013
- Medeiros J., Contaldi C. R., 2006, *MNRAS*, 367, 39
- Moss I., Xiong C., 2007, *JCAP*, 0704, 007
- Munshi D., Heavens A., 2010, *MNRAS*, 401, 2406
- Munshi D., Souradeep T., Starobinsky, Alexei A., 1995, *ApJ*, 454, 552
- Munshi D., Melott A. L., Coles P., 2000, *MNRAS*, 311, 149
- Munshi D., Heavens A., Cooray A., Smidt J., Coles P., Sema P., 2009, preprint (arXiv:0910.3693)
- Salopek D. S., Bond J. R., 1990, *Phys. Rev. D*, 42, 3936
- Salopek D. S., Bond J. R., 1991, *Phys. Rev. D*, 43, 1005
- Santos M. G. et al., 2003, *MNRAS*, 341, 623
- Seery D., Lidsey J. E., Sloth M. S., 2007, *JCAP*, 0701, 027
- Smidt J., Amblard A., Serra P., Cooray A., 2009, *Phys. Rev. D*, 80, 123005
- Smidt J., Amblard A., Cooray A., Heavens A., Munshi D., Serra P., 2010, preprint (arXiv:1001.5026)
- Smith K. M., Zaldarriaga M., 2006, preprint (arXiv:astro-ph/0612571)
- Smith K. M., Zahn O., Dore O., 2007, *Phys. Rev. D*, 76, 043510
- Smith K. M., Senatore L., Zaldarriaga M., 2009, *JCAP*, 0909, 006
- Spergel D. N., David M., Goldberg D. M., 1999a, *Phys. Rev. D*, 59, 103001
- Spergel D. N., David M., Goldberg D. M., 1999b, *Phys. Rev. D*, 59, 103002
- Spergel D. N. et al., 2007, *ApJS*, 170, 377
- Szapudi I., Szalay A. S., 1999, *ApJ*, 515, L43
- Yadav A. P. S., Wandelt B. D., 2008, *Phys. Rev. Lett.*, 100, 181301
- Yadav A. P. S., Komatsu E., Wandelt B. D., 2007, *ApJ*, 664, 680
- Yadav A. P. S., Komatsu E., Wandelt B. D., Liguori M., Hansen F. K., Matarrese S., 2008, *ApJ*, 678, 578

This paper has been typeset from a \LaTeX file prepared by the author.